

**ASSESSMENT OF ENVIRONMENTAL IMPACT FOR
ACCIDENTAL RELEASE OF HEAVY GAS**

Yasanthi Nadun Gunawardena

Index No: 119257A

Thesis/Dissertation submitted in partial fulfillment of the requirements for the degree
Master of Science

Department of Chemical and Process Engineering

University of Moratuwa

Sri Lanka

June 2016

Declaration, copyright statement and the statement of the supervisor

I declare that this is my own work and without acknowledgement this thesis/dissertation does not incorporate any material previously submitted for a Degree or Diploma in any other University or institute of higher learning and to the best of my knowledge and belief it does not contain any material previously published or written by another person except where the acknowledgement is made in the text.

Also, I hereby grant to University of Moratuwa the non-exclusive right to reproduce and distribute my thesis/dissertation, in whole or in part in print, electronic or other medium. I retain the right to use this content in whole or part in future works (such as articles or books).

.....

Y. N. Gunawardena

.....

Date

The above candidate has carried out research for the Masters Dissertation under my supervision.

.....

Supervisor:

Dr. (Ms) M.Y. Gunasekera

.....

Date

.....

Supervisor:

Dr. M. Narayana

.....

Date

Abstract

An air dispersion model can be used to mathematically simulate air pollutants dispersion in the ambient atmosphere. These dispersion results can be used to predict their environmental impact, concentrations and movement. Such predicted data of hazardous gases released after a chemical accident are valuable since it can be used to provide timely information to emergency response providers as well as to make decisions on siting chemical plants at safe distances from settlements during plant development stages.

Dense gas dispersion is the focus of this research as several pressurized dense gas release accidents have happened during the last few years in this country. These gases form clouds heavier than air when released to the atmospheric environment. In this study a mathematical model for the dispersion of heavy gas due to an accidental release is presented in order to determine the environmental impact.

The heavy gas model was then used to simulate the dispersion of negatively buoyant and highly toxic chlorine gas to illustrate the use of heavy gas dispersion modeling in hazard analysis. A worst case scenario study with stability class A, was used for an accidental release of 900kg of chlorine from a location in Kaluthara district in Sri Lanka. To determine the impact of the release probit analysis, safe distance and hazardous time period calculations were done. From the model results, for a 900kg chlorine release, safe Immediately Dangerous to Life or Health (IDLH) distance was above 490m. Within this hazardous zone the safe time period starts after 5.44 minutes from the release. Further, this model can be used to predict information, such as concentration variation of the substance released with time and, cloud dimensions such as height and radius. For validation, experimental data in literature were collected and a sensitivity analysis was done to identify the best values for the model parameters.

Key-words: Dense gas dispersion, environmental impact, chlorine, accidental release, safe distance

Acknowledgement

I would like to extend my sincere gratitude to my supervisors, Dr. M. Y. Gunasekera for her valuable guidance, advice and support extended in this study, and Dr. M. Narayana for the kind supervision given while assisting as the M.Sc. coordinator of the Post Graduate Division of the Chemical and Process Engineering department.

Also I would like to thank the administrative officers of M.Sc./PGD in Sustainable Process Development, University of Moratuwa for the timely information given regarding the research work.

In addition, I am grateful to my colleagues who helped me in many ways such as collecting and analyzing data. Special appreciation is given to my family for their immense support.

Finally, I would like to thank each and every one who came across this research for making this study a success.

Table of Content

Declaration, copyright statement and the statement of the supervisor	i
Abstract	ii
Acknowledgement	iii
Table of Content	iv
List of Figures	vi
List of Tables	vii
List of Appendices	vii
1 INTRODUCTION	1
1.1 Importance of Dense Gas Dispersion Modeling	1
1.2 Objectives and Scope	3
2 LITERATURE SURVEY	4
2.1 Historical Background	4
2.2 Dense Gas Dispersion	6
2.3 Dense Gas Dispersion Process	8
2.4 Classification of Heavy Gas Dispersion Models	9
2.4.1 Box model	9
2.4.2 Plume model	10
2.4.3 Puff model	11
2.5 Impact Assessment Methodology	11
2.5.1 Input data collection	12
2.5.2 Dispersion modeling	13
2.5.3 Processing dispersion model output data	13
2.5.4 Interpretation of dispersion modeling results	14
2.5.4.1 Use of Probit functions	14
2.5.4.2 Determination of harmful dose	16
3 MODEL FORMULATION	18
3.1 Model Assumptions	18
3.2 Gravitational Slumping	20
3.3 Entrainment of Air	20
3.4 Transition to the Passive Phase	21

3.5	Density of the Cloud -----	22
3.6	Concentration Profile -----	22
3.7	Model Equations-----	23
3.8	Numerical Simulation of Model Equations -----	25
3.9	Case Study of Heavy Gas Release -----	25
3.9.1	Properties of Chlorine gas -----	26
3.9.2	Input data to the model-----	28
3.9.2.1	Meteorological data -----	28
3.9.2.2	Release height -----	29
3.9.2.3	Terrain and sensitive receptors -----	30
3.9.2.4	Building wake effects -----	30
3.10	Calculation-----	31
3.10.1	Gravity slumping phase-----	31
3.10.2	Air entrainment phase-----	32
3.10.3	Post transition phase-----	36
3.11	Numerical Simulation-----	36
3.12	Model Validation -----	36
3.13	Interpretation of Dispersion Modeling Results -----	40
4	RESULTS AND DISCUSSION	41
4.1	Numerical Simulation Results -----	42
4.2	Radius and Height Variation with Time-----	42
4.2.1	Gravity slumping phase-----	42
4.2.2	Air entrainment phase-----	44
4.2.3	Post transition phase-----	48
4.3	Concentration Profile -----	50
4.4	Safe Downwind Distance and Critical Time Interval -----	52
4.5	Probit Analysis of Model Results -----	53
5	CONCLUSIONS.....	54
5.1	Recommendations for future work-----	55
	REFERENCES	56

List of Figures

Figure 2.1 Different phases in the dispersion of heavy gas clouds.....	8
Figure 2.2 Box model	10
Figure 2.3 Buoyant Gaussian air dispersion plume	10
Figure 2.4 Puff model	11
Figure 2.5 Probit analyses for chlorine death	15
Figure 2.6 Probit analyses for chlorine injury.....	16
Figure 3.1 Cylindrical cloud geometry	19
Figure 3.2 Effects of exposure to different concentrations of chlorine	26
Figure 3.3 Model validation data points	39
Figure 4.1 Site layout of the case study	41
Figure 4.2 Variation of cloud radius with time during gravity slumping phase	43
Figure 4.3 Variation of cloud height with time during gravity slumping phase.....	44
Figure 4.4 Variation of cloud radius with time during air entrainment phase.....	45
Figure 4.5 Variation of cloud height with time during air entrainment phase.....	46
Figure 4.6 Variation of entrained air mass with time during air entrainment phase..	47
Figure 4.7 Variation of radius during post transition phase.....	48
Figure 4.8 Variation of height during post transition phase	48
Figure 4.9 Variation of radius and height during all three phases	49
Figure 4.10 Concentration profile at different times after the release	50
Figure 4.11 Propagation of contours in downwind direction.....	51
Figure 4.12 Safe IDLH distance and critical time period for different chlorine releases.....	52

List of Tables

Table 2.1 List of gases with densities	7
Table 2.2 Probit equations for chlorine exposure	15
Table 3.1 Model Equations used in the simulation.....	24
Table 3.2 Properties of chlorine.....	26
Table 3.3 The concentrations of chlorine tolerable and intolerable to man.....	27
Table 3.4 Pasquill stability classes.....	28
Table 3.5 Meteorological conditions affecting atmospheric stability class	29
Table 3.6 Input data used in the model	30
Table 3.7 Experimental data in Thorney Island Trial 008	38
Table 3.8 Observed and predicted maximum concentrations at various downwind distances in Thorney Island Trial 008.....	38
Table 4.1 Safe downwind distances and Critical time intervals based on IDLH value	52

List of Appendices

Appendix – A Supporting calculation excel for the Matlab m files.....	58
Appendix – B mfile for entrainment phase	59
Appendix – C mfile for post transition period	62
Appendix – D mfile for all three phases	65
Appendix – E mfile for concentration profile	68
Appendix – F m file for contour curves	72
Appendix – G Probit calculation Excel sheet	75
Appendix – H Model validation and sensitivity analysis of parameters	78

1 INTRODUCTION

In order to prevent and mitigate industrial accident consequences, modeling releases of hazardous or toxic gases has become a rapidly evolving field, driven by the efforts of the industry, as well as public concern that is beginning to be reflected in regulatory requirements. Air dispersion models are often used in environmental impact assessments, land use planning in siting industries, emergency planning, risk analysis and source distribution studies. Although these models are seen used in environmental impact assessment and risk assessment studies in Sri Lanka (for e.g. EIA done at AES Kelanitissa Power Plant in year 2000 [1]), use of them in industrial land use planning and emergency response planning are rare.

Atmospheric dispersion modeling done mathematically is able to simulate how gases or air pollutants disperse in the ambient atmosphere. A dispersion model is therefore used for predicting concentrations in downwind distance of a pollutant released continuously from a source such as industrial plants, vehicular traffic or released instantaneously from an accident. The dispersion model is therefore designed based on the knowledge of these emission characteristics as well as the nature of terrain and state of the atmosphere. The model has to be able to predict rates of dispersal based on measurable meteorological variables such as wind speed, atmospheric turbulence, and thermodynamic effects. The algorithms at the core of air pollution models are based upon mathematical equations describing these various phenomena which, when combined with empirical or field data, can be used to predict concentration distributions downwind of a source.

1.1 Importance of Dense Gas Dispersion Modeling

Most of the severe accidents which have occurred in the process industry and which are documented in the literature in the past are associated with the dispersion of a dense gas cloud. Some examples are given below;

- Blair, Nebraska, USA[2] - This accident occurred in 1970, where a very large tank of liquefied ammonia was overfilled. Over a period of two hours, a total of 160 tons of ammonia was released. The accident had occurred at a remote location and no human fatalities resulted.
- Houston, Texas, USA [2] - In this accident, which happened in 1976, a complete failure of a road tanker containing 19 tonnes of ammonia resulted after the tanker had fallen from an elevated roadway. There had been a rapid formation of a large cloud which slumped to ground level and spread over the surrounding area. Six people were killed.
- Bhopal, India [2] – This accident occurred on December 1984 at the Union Carbide India Limited (UCIL) which is a pesticide plant in Bhopal, Madhya Pradesh. Over 500,000 people were exposed to methyl isocyanate (MIC) gas and other chemicals, and reports of government of Madhya Pradesh indicated 3,787 deaths and 558,125 injuries [2].
- Graniteville, South Carolina [3] - On January 6, 2005, a freight train holding a pressurized tanker carrying chlorine gas was involved in a collision in Graniteville, South Carolina. This collision had released nearly 70 tons of chlorine gas into the surrounding area, resulting nine fatalities, over 500 injuries, and over 5,000 evacuations.
- Chlorine leak at Paranthan Chemicals Company Ltd. [4] –In Sri Lanka an accident is reported where, Chlorine leak had taken place at the Fullerton Industrial Zone in Nagoda, Kalutara, leaving 11 people including three employees injured [4].

Therefore, modeling of dispersion of the ‘dense’ gases has become important to avoid such harmful consequences as described in the above accidents. As heavy gases tend to disperse downwards on earth surface the release of these gases will involve a high probability of human beings being affected and/or ignition sources being encountered.

A heavier-than-air gas cloud tends to fall to the ground due to its negative buoyancy and to remain there at usually high levels of concentration for comparatively long periods as opposed to neutral or positively buoyant clouds. As a consequence a

heavy gas cloud can travel over considerable distances threatening a wider area at ground level compared to neutrally buoyant clouds. Therefore the significance of heavier-than-air gases is evident in terms of safety and accident prevention.

1.2 Objectives and Scope

The objectives of this study are to,

- Develop a mathematical model for the dispersion of accidental release of heavy gas in the atmosphere.
- Use the model developed to determine the impact on the environment
- Apply the model and determine the environmental impact in a case study

There are two scenarios for the time aspect of a dense gas release that is being instantaneous or continuous. In an accidental release the quantity of the heavy gas is released instantaneously. Therefore, for the modeling of accidental release, an instantaneous release is considered in the scope of this work. The accidental releases of gases observed in past incidents are mainly from ground level sources. Therefore, in the scope of this work a ground level heavy gas instantaneous release is considered.

2 LITERATURE SURVEY

2.1 Historical Background

Bosanquet [1957] proposed one of the first significant models for plumes heavier than air. In his paper, a theoretical model initially proposed for the dispersion of a stack plume lighter than air has been modified.

Ooms [1972] provided a much more realistic description of the dispersion of a heavy cloud. They proposed an analytical model based on using the conventional transport phenomena and the plume path theory by Ooms [1972]. In contrast with the earlier models, Ooms approach allowed for the treatment of plumes with temperature different from the atmospheric temperature. A disadvantage of the model was that the plume's cross section was assumed circular, contrary to the experimental results that indicate that in general it is elliptical. Ooms and Duijm [1984] corrected this in a later paper.

Consequently many new models were proposed using the so-called “Top Hat” or “Slab” and “K-theory” or “Eddy diffusivity” approaches. One of the first “Top Hat” approaches to modeling was that of Van Ulden [1974]. “Top Hat” model assumes that mass transfer occurs by entrainment across the density interface of a cloud with an assumed shape (e.g. cylindrical) and that internal mixing is fast enough for the concentration within the cloud to be uniform.

Later Colenbrander [1980] proposed slab (continuous release box) model which assumes normal distribution of concentration within the slab. Development of this model by Colenbrander led to the design of the popular model known as HEGADAS (Spicer and Havens [1986]). The model improved the way in which the influence of density gradients was taken into account on the dispersion in the vertical direction. In addition it introduced a description of crosswind spreading of the plume under gravity. The model initially did not treat aerosols and was applicable only to continuous releases. The earliest version was included as part of the HGSYSTEM, which now accounts for vapor-liquid equilibrium in an explicit way.

Around the same time Eidsvik [1980] proposed a refined box model with equations modified to estimate vertical entrainment of air.

In 1985 Van Ulden and Holtslag used K-theory with atmospheric scaling parameters to model heavy gas dispersion. K-theory models numerically integrate suitably simplified equation of mass, momentum and energy conservation in two or three dimensional form.

Ermak and Chan [1985] proposed a model based on the turbulence dissipation and boundary layer parameters. In subsequent years, Langlo and Schatzmann [1991] modeled the heavy gas dispersion using Lagrangian approach based on similarity theory. Deaves [1992] modeled the atmospheric turbulence and analyzed the way it affects dense gas dispersion. He also used K-theory and employed more extensive meteorological data than the other models for wind profile, turbulence and boundary layer profiles.

Many models have been developed in the last ten years as a development of the earlier models. Their main difference lies on the assumptions taken to solve the fundamental equations of motion, the correlations used to model the transport of the cloud, or the treatment of specific systems (e.g. aerosols, continuous/instantaneous releases, high pressure/low pressure, etc).

U.S. Environmental Protection Agency (U.S. EPA) has accepted many of these models developed to be used in many other countries as well. Those EPA recommended models are as follows [22];

- AERMOD - An atmospheric dispersion model based on atmospheric boundary layer turbulence structure and scaling concepts, including treatment of multiple ground-level and elevated point, area and volume sources. It handles flat or complex, rural or urban terrain and includes algorithms for building effects and plume penetration of inversions aloft.
- CALPUFF - A non-steady-state puff dispersion model that simulates the effects of time- and space-varying meteorological conditions on pollution transport, transformation, and removal. CALPUFF can be applied for long-range transport and for complex terrain.

- BLP - A Gaussian plume dispersion model designed to handle unique modeling problems associated with industrial sources where plume rise and downwash effects from stationary line sources are important.
- CALINE3 - A steady-state Gaussian dispersion model designed to determine pollution concentrations at receptor locations downwind of highways located in relatively uncomplicated terrain.
- CAL3QHC and CAL3QHCR - CAL3QHC is a CALINE3 based model with queuing calculations and a traffic model to calculate delays and queues that occur at signalized intersections.
- CTDMPLUS - A Complex Terrain Dispersion Model (CTDM) plus algorithms for unstable situations (i.e., highly turbulent atmospheric conditions). It is a refined point source Gaussian air quality model for use in all stability conditions (i.e., all conditions of atmospheric turbulence) for complex terrain.
- OCD - Offshore and Coastal Dispersion Model (OCD) is a Gaussian model developed to determine the impact of offshore emissions from point, area or line sources on the air quality of coastal regions.

2.2 Dense Gas Dispersion




Many conditions, including high molecular weight, low temperatures, chemical transformations, and aerosol formation can lead to heavier-than-air clouds. Britter gives four categories of dense gases, which can be summarized as follows [5]:

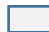

1. Gases with higher molecular weight than the surrounding air.
2. Gases with a lower molecular weight than the surrounding air, but with a relatively low temperature, resulting in a higher density;
3. Gases with droplets, which increase the gas cloud's density. The droplets are often a result of the release scenario; and
4. Gases which react with the water in the atmosphere resulting in a heavy composition.

The Table 2.1 below illustrates the gases which fall into dense gas category [6];

Table 2.1 List of gases with densities

Substance	Formula	Relative Density	Form
Hydrogen	H ₂	0.07	Gas
Helium	He	0.14	Gas
Methane	CH ₄	0.55	Gas
Ammonia	NH ₃	0.59	Gas
Hydrogen Fluoride	HF	0.69	Gas
Acetylene	C ₂ H ₂	0.90	Gas
Hydrogen Cyanide	HCN	0.93	Vapor
Carbon Monoxide	CO	0.97	Gas
Nitrogen	N ₂	0.97	Gas
Ethylene	C ₂ H ₄	0.97	Gas
Air at 20 °C/68 °F	-	1.00	Gas
Formaldehyde	HCHO	1.04	Gas
Nitrogen Monoxide	NO	1.04	Gas
Ethane	C ₂ H ₆	1.04	Gas
Air at 0 °C/ 32 °F	-	1.07	Gas
Methanol	CH ₃ OH	1.10	Vapor
Oxygen	O ₂	1.10	Gas
Phosphine	PH ₃	1.17	Gas
Hydrogen Sulfide	H ₂ S	1.18	Gas
Hydrogen Chloride	HCl	1.26	Gas
Fluorine	F ₂	1.31	Gas
Propylene	C ₃ H ₆	1.45	Gas
Ethylene Oxide	C ₂ H ₄ O	1.52	Gas
Carbon Dioxide	CO ₂	1.52	Gas
Propane	C ₃ H ₈	1.52	Gas
Nitrogen Dioxide	NO ₂	1.59	Vapor
Methyl chloride	CH ₃ Cl	1.74	Gas
Acrylonitrile	CH ₂ CHCN	1.83	Vapor
Acrolein (Acryl aldehyde)	C ₂ H ₃ CHO	1.94	Vapor
n-Butane	C ₄ H ₁₀	2.01	Gas
Sulfur Dioxide	SO ₂	2.21	Gas
Chlorine	Cl ₂	2.45	Gas
Benzene	C ₆ H ₆	2.70	Vapor
Hydrogen Bromide	HBr	2.79	Gas
Phosgene	COCl ₂	3.41	Gas
Bromine	Br ₂	5.52	Vapor

-  Buoyant gases
-  Neutral gases
-  Dense gases

-  Vapor
-  Reference

2.3 Dense Gas Dispersion Process

When the dispersed vapor cloud is heavier than air (negatively buoyant), cloud will eventually hit the ground after being released.

As shown in Figure 2.1, a dense-gas release can be divided into several stages characterized by a dispersing mechanism: (1) initial acceleration and dilution, (2) internal buoyancy dominance, (3) Transition and (4) passive dispersion or dominance of ambient turbulence [7].

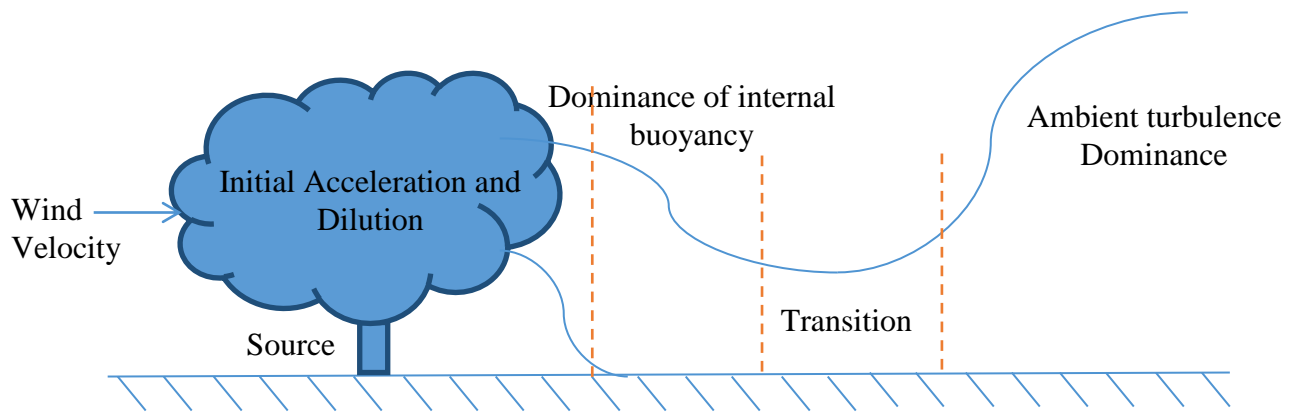


Figure 2.1 Different phases in the dispersion of heavy gas clouds

(1) Initial acceleration and dilution;

In the first stage, the mode of storage and type of rupture that caused the release dominate the behavior. In catastrophic failures from pressurized vessels there will be a rapid flash of the stored liquid. The sudden expansion to ambient pressure provokes the evaporation of superheated liquid, followed by an immediate formation of liquid droplets and the development of two-phase flow.

(2) The initial gravity dominated or slumping phase;

The density difference between the cloud and the ambient air results in gravitational slumping and cloud height decreases and radius increases. In this phase, the turbulence resulted from gravitational slumping dominates the cloud figure dimension, entrainment of air and concentration distribution in the cloud. In this phase atmosphere turbulence is a minor factor.

(3) The transition phase;

The process of entrainment of air is the process of cloud dilution. As the cloud is diluted the density difference becomes smaller and smaller. As it moves downwind, gravity causes spread.

(4) The buoyancy dominated phase.

Farther downwind, cloud becomes more dilute and behaves like neutrally buoyant gas. As the density difference is smaller than the critical value, effect of heavy gas can be regarded as disappearing completely. In this phase atmospheric turbulence dominates the dispersion.

2.4 Classification of Heavy Gas Dispersion Models

There are three general types of dispersion models, namely box, plume, and puff. Box model is conceptually the simplest although some relatively complex models have been built on box model foundations. These three types form the basis of almost all dispersion simulations which are in use today.

In addition to these three types, some very complex models have been developed that attempt to solve the basic physical equations of motion of the air parcels without using the approximations of the box, plume, or puff models.

2.4.1 Box model

The box model is called a box model for obvious reasons. The region is approximated as having definite sides and a lid as well as a flat bottom at ground level as shown in figure 2.2. The flow of air is assumed to be in one end and out the other. The sources within the box are modeled as a completely mixed and dispersed area source. Therefore the box model estimates the average concentration of the plume (or sum of plumes) at all points on downwind face.

The calculations for box model are straight forward and useful for those approximations which can help define a problem. The limitations are obvious. Urban emissions from point and line sources do not get uniformly back mixed with in a

clearly defined volume. At certain places within the box, the pollution level would be much higher or much lower than that calculated [8].

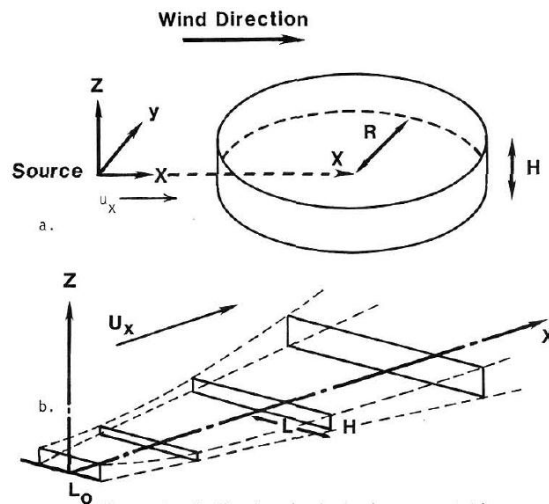


Figure 2.2 Box model

2.4.2 Plume model

Plume models use a more realistic description of dispersion. With realism, unfortunately, comes complexity. With a plume model it is possible to treat sources individually rather than combining them as in the box model. As plume moves downwind it spreads vertically and horizontally as shown on figure 2.3. The concentration varies in space. The total concentration at a receptor point is the sum of the contributions from all sources plus the background concentration [8].

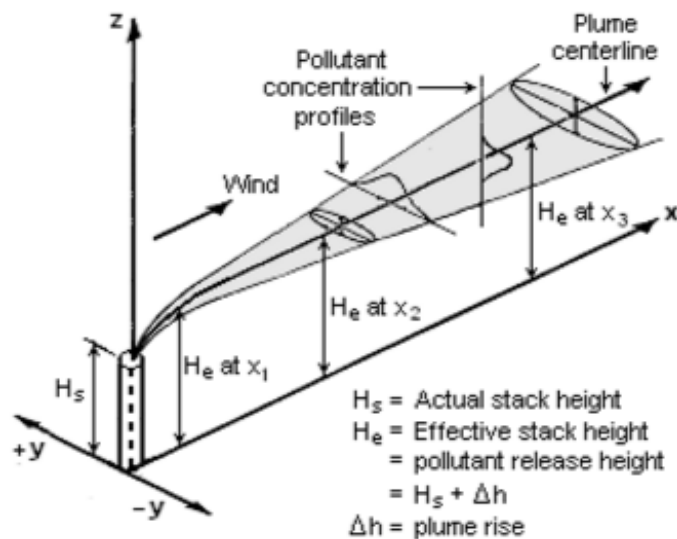


Figure 2.3 Buoyant Gaussian air dispersion plume

2.4.3 Puff model

The final basic model type to be considered is the puff model. Here the emissions are treated as the individual puffs as shown on figure 2.4. This is a model which includes time variables. Otherwise application of the puff model is similar to that of the plume model. The time considerations and the different nature of the puff equation make it difficult and expensive to apply to a complex multiple source regions, unless large core, low cost computer facilities are available [7].

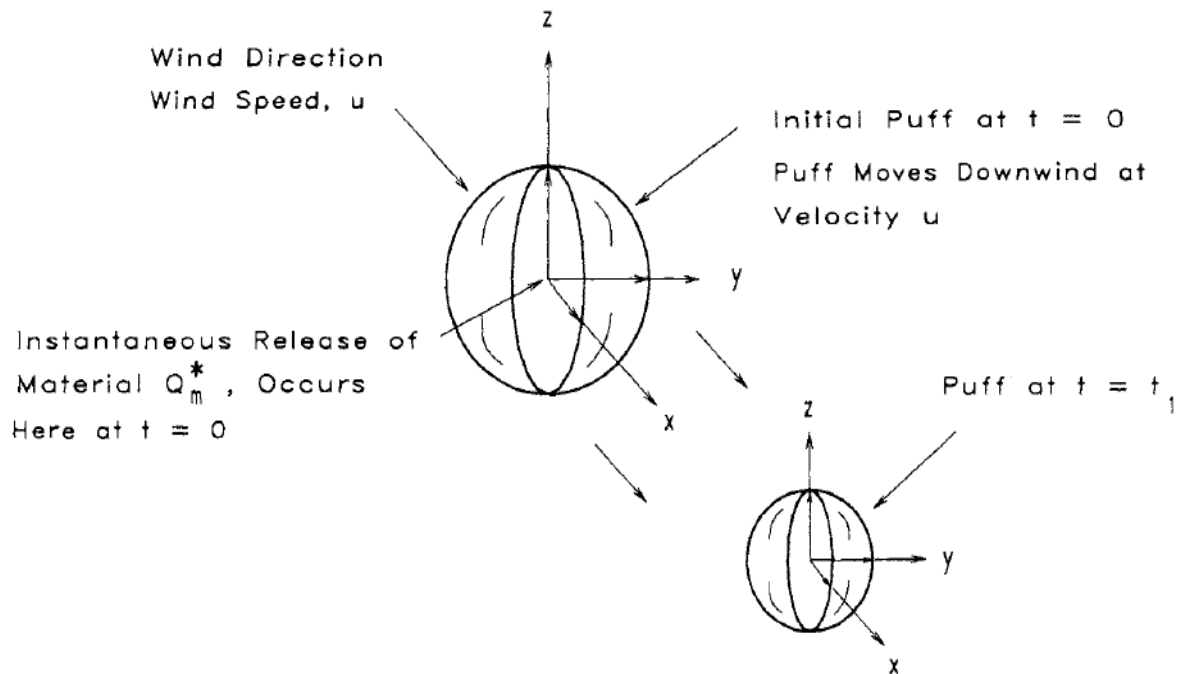


Figure 2.4 Puff model

2.5 Impact Assessment Methodology

There are four main stages in an air quality impact assessment using dispersion data [9];

1. Input data collection
2. Dispersion modeling
3. Processing dispersion model output data
4. Interpretation of dispersion modeling results

2.5.1 Input data collection

The first stage in the impact assessment is the collection of all the information required to complete the dispersion modeling [9].

The required input of data may include:

1. Type of emission sources

- Point source - A point source is a stationary, single specific source of emissions (E.g: combustion furnace flue gas stack), which has no geometric dimensions.
- Line sources- A line source is one-dimensional source of emission to the atmosphere that is distributed over a line such as conveyor belts, roadways, and rail lines. A line source becomes an area source if the breadth exceeds 20% of the length.
- Area source - An area source is a two-dimensional source of diffuse emissions. (For example, emissions from a forest fire, a landfill or the evaporated vapors from a large spill of volatile liquid).
- Volume source – A volume source is a three-dimensional source of diffuse emissions. (E.g; the fugitive gaseous emissions from piping flanges, valves and other equipment at various heights within industrial facilities such as oil refineries and petrochemical plants).

Other air pollutant emission source characterizations;

- Stationary or mobile sources. Flue gas stacks are examples of stationary sources and vehicles are examples of mobile sources.
- Sources characterized as either urban or rural. Since urban areas constitute a so-called heat island and the heat rising from an urban area causes the atmosphere above an urban area to be more turbulent than the atmosphere above a rural area.
- Sources characterized by their elevation. Relative to the ground as either surface or ground-level, near surface or elevated sources.
- Sources characterized by their time duration. For example puff or intermittent, short term sources and continuous: a long term source (E.g; flue gas stack emissions)

2. Meteorological conditions such as wind speed and direction
 - Wind speed (m/s)-This dilutes the plume in the direction of transport and determines the travel time from source to receptor. As the wind speed increases, the substance is carried downwind faster but is diluted faster by a larger quantity of air.
 - Wind direction (°) – This determines the initial direction of transport of pollutants from their sources.
3. The amount of atmospheric turbulence (as characterized by what is called the "stability class"), the ambient air temperature, cloud cover and solar radiation.
4. Source characterization and temperature of the material
5. Emissions or release parameters such as source location and height, type of source (i.e., fire, pool or vent stack) and exit velocity, exit temperature and mass flow rate or release rate.
 - Terrain elevations at the source location and at the receptor location(s), such as nearby homes, schools, businesses and hospitals.
 - The location, height and width of any obstructions (such as buildings or other structures), surface roughness of terrain.

2.5.2 Dispersion modeling

After gathering the input data, a model is developed to describe how materials are discharged from the process. The source model provides a description of the rate of discharge, the total quantity or time of discharge, and the state of the discharge. A dispersion model is subsequently used to describe how the material is transported downwind and dispersed to some concentration levels.

2.5.3 Processing dispersion model output data

Next stage of the assessment process is the calculation of ground-level concentrations of pollutants in the region surrounding the premises. This output may contain the model characteristics such as height, radius, density, entrained air mass etc. Hazardous zones can be identified by calculating the safe downwind distances and critical time intervals.

2.5.4 Interpretation of dispersion modeling results

The final stage of the impact assessment is the interpretation of the dispersion modeling results.

In order to estimate the effects of the toxic release, it is therefore necessary to know the relationships between the concentration profile and the degree of injury. A toxic release will have an effect on human life in one of the following ways, such as,

- Lethal injury (death),
- Non-lethal injury
- Irritation

There are two main approaches for the determination of the effects of received dose:

1. Use of Probit functions
2. Determination of harmful dose

2.5.4.1 Use of Probit functions

The degree of variation in dose-response can be presented in the form of a Gaussian response, which was expressed by Eisenberg as a probit equation [10].

Probits account for the variation in tolerance to harm for an exposed population. The fatality rate of personnel exposed to harmful agents over a given period of time can be calculated by the use of probit functions that typically take the form [10]:

$$Y = k_1 + k_2 \ln(C^n t) \quad (2.1)$$

Where:

Y = probit, (value range 2.67 – 8.09 representing 1 – 99.9% fatality) a measure of the percentage of the vulnerable resource that might sustain damage. Fatality probability can then be determined by evaluation of Y on a probit transformation calculation. (See Appendix G)

$k_1 + k_2 = \text{Constants}$

C = hazard concentration (ppm) to an exponent “n”

t = time in minutes

The probit equations for chlorine deaths and injuries are presented in Table 2.2 [11].

Table 2.2 Probit equations for chlorine exposure

Equation for Fatality				
		Lethal Conc. for 30 minute Exposure period (ppm)		
		LC ₁₀	LC ₅₀	LC ₉₀
Eisenberg, Lynch and Breeding [11]	$Y = -17.1 + 1.69\ln(\Sigma C^{2.75}t)$	26	34	44
Equation for Injury				
Eisenberg, Lynch and Breeding; Perry and Articola [11]	$Y = -2.40 + 2.90 \ln(C)$			

Source: F. Lees, *Loss prevention in the process industries*. London: Butterworths.

The responses to a given dose are presented by two cumulative graphs (probit curves), Figure 2.5 and Figure 2.6, which indicate the probabilities of percentage deaths and injuries for a specific dose and exposure time, respectively.

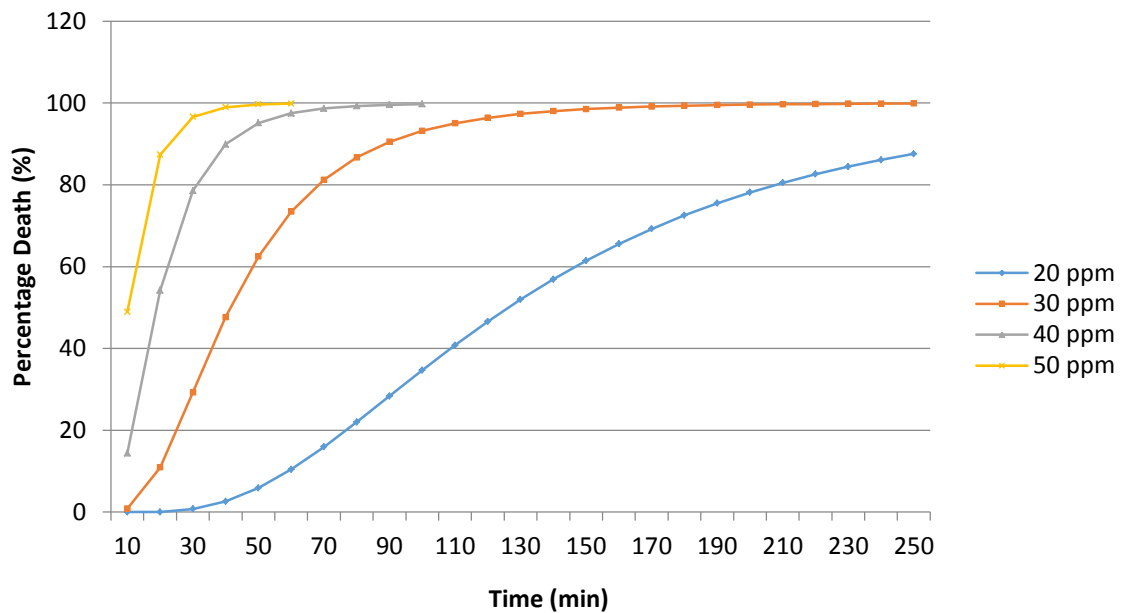


Figure 2.5 Probit analyses for chlorine death

According to the above figure it could be seen, when the exposed concentration is increased, the time of exposure for 100% death is decreased. i.e. for 30ppm it is 4 hours and 20 minutes and for 50ppm it is 1 hour. 0.

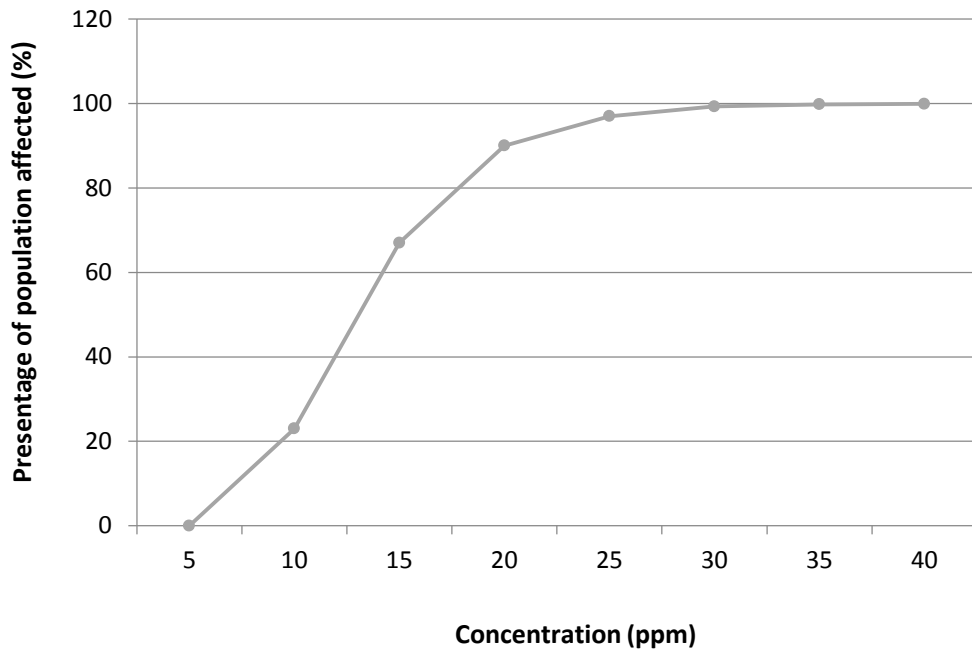


Figure 2.6 Probit analyses for chlorine injury

Non-lethal injury is taken to mean hospitalization with or without lasting impairment of health. For non-lethal injuries, according to Figure 2.5, 37 ppm concentration will affect 100% of people.

2.5.4.2 Determination of harmful dose

The designation harmful dose is used to indicate the dose (exposure) that will produce signs of toxicity in a certain percentage of test species.

One of the more commonly used measures of toxicity is the LD50. The LD50 (the lethal dose for 50 percent of the animals tested) of a chemical is usually expressed in milligrams of chemical per kilogram of body weight (mg/kg). The TLV (threshold

limit value) for a chemical is the airborne concentration of the chemical (expressed in ppm) that produces no adverse effects in workers exposed for eight hours per day five days per week. The TLV is usually set to prevent minor toxic effects like skin or eye irritation.

Immediately Dangerous to Life or Health (IDLH) value is a quantitative assessment of the potential risk associated with the exposure of that toxic chemical. It represents the maximum concentration from which, in the event of a respiratory failure, one could escape in 30 minutes without a respirator and without experiencing any escape impairing or irreversible health effect [12]. Since chlorine is a toxic gas which poses an immediate threat to health or life, IDLH value is considered in determination of the potential risk associated in a release.

3 MODEL FORMULATION

This study undertakes the development of a simple heavy gas dispersion model which could be used for environmental impact assessment. It is a numerical dense gas model which includes all the basic features plausible to dense gas dispersion in a realistic manner.

The model in the present study has been developed taking into account the work carried out by Singh [1990], Mohan [1993], Van Ulden [1974], Eidsvik [1980], Cox and Carpenter [1979], and several other persons.

3.1 Model Assumptions

1. Dense gas release was assumed to take place due to a catastrophic failure of a pressurized vessel. Release from a catastrophic failure of a vessel can be considered as a typical dense gas release scenario, which was generally modeled by taking the source term as a cylindrical cloud.
2. Radius and height of the cylindrical volume was considered as equal at time $t = 0$ s.
3. It was assumed that the initial stages of dispersion could be described by a modified box model type and the atmospheric dispersion stage could be described using a modified Gaussian, volume source based model.
4. In this model all properties (concentration, density, absolute temperature etc.) were assumed to be uniformly distributed within this volume.
5. Toxic mass has a Gaussian distribution in concentration profile.
6. Common features of a simplest situation of a box model are considered here, namely instantaneous release at time $t = 0$ of a finite initial volume V_0 of heavy gas, of uniform initial density ρ_0 .
7. The heavy gas was assumed to be released from a vessel located on the ground. Hence the height of release was taken to be at ground level.
8. Dispersion process was considered to be isothermal and the ambient atmosphere to be neutrally stratified.
9. As the temperature of the releasing substance, air and ground are the same, cloud heating was neglected.

10. Local mean fluctuations of concentration and possible two phase flashing flow are assumed to be negligible.

The dense gas cloud from an instantaneous release was approximated by a cylinder of radius, height and volume r , h and V respectively as shown in Figure 3.1.

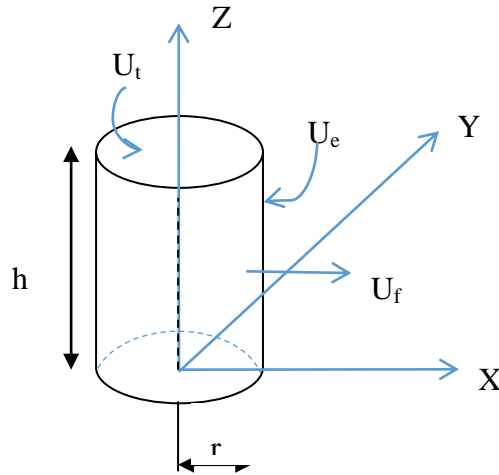


Figure 3.1 Cylindrical cloud geometry

Hence volume of cloud is given by equation (3.1);

$$V = \pi r^2 h \quad (3.1)$$

Where;

- r = the cloud radius
- h = cloud height
- V = cylinder volume

The radius grows with a front velocity U_f , and the center of mass x moves with the advection velocity u .

The horizontal spreading equation is given by equation (3.2);

$$\frac{dr}{dt} = U_f \quad (3.2)$$

The characteristic features of dense gas dispersion included in the model gravity slumping, air entrainment and transition to passive phase are as discussed in the following section.

3.2 Gravitational Slumping

The box models assume that the rate of spreading of the cloud about its axis, namely $\frac{dr}{dt}$, is proportional to the excess hydro static pressure at the base of the cloud, which is calculated by the following equation (3.3) [11];

$$\frac{dr}{dt} = C \sqrt{gh \frac{(\rho_g - \rho_a)}{\rho_g}} \quad (3.3)$$

Where;

t - Time when gravity slumping has started,

g - Gravitational acceleration,

ρ_g - Density of chlorine within the cylinder

ρ_a - Density of air within the cylinder

C – Constant

3.3 Entrainment of Air

The gradual increase of the cloud mass is modeled by an entrainment velocity U_e from the top cloud interface, and the enhanced mixing at the front is modeled by the edge entrainment velocity.

The rate at which air is entrained into the cloud is given by equation (3.4) [11]:

$$\frac{dM_a}{dt} = \rho_a(\pi r^2)U_e + 2\rho_a(\pi r h)\alpha^* \left(\frac{dr}{dt}\right) \quad (3.4)$$

Where;

M_a – Entrained mass of air

α^* - Parameter which controls the rate of edge entrainment of air

U_e - Top entrainment velocity

The top entrainment velocity U_e is a function of Richardson number R_i and the longitudinal turbulence velocity U_l , which is given by the equation (3.5);

$$U_e = \alpha' U_l R_i^{-1} \quad (3.5)$$

Different Richardson numbers are in general used in a lot of applications concerning dense gas dispersion. The Richardson number used in this model is given by equation (3.6);

$$R_i = \left(\frac{g l_s}{U_l^2} \right) \frac{(\rho_g - \rho_a)}{\rho_g} \quad (3.6)$$

Where;

l_s – Turbulence length scale

The turbulence length scale is a function of the height above the ground and of stability which is given by the following equation (3.7) [11];

$$l_s = 5.88 h^{0.48} \quad (3.7)$$

3.4 Transition to the Passive Phase

As the cloud travels downstream, it will find a final phase where its velocity is near or below the wind velocity and its density is insignificantly different from that of the atmosphere. Dense gas release eventually progresses to a stage where the normal atmospheric mixing processes become dominant and the dispersion enters the passive phase.

After transition of the cloud to the passive phase, cloud dimensions are taken as equations (3.8) and (3.9) [11];

$$r = r_T + 2U_*(t - t_T) \quad (3.8)$$

$$h = h_T + \alpha'' U_*(t - t_T) \quad (3.9)$$

Where;

α'' - coefficient for vertical entrainment with a value of 0.4

r_T and h_T - the radius and height at the time of transition

U_* - the friction velocity due to mechanical turbulence

t –time

3.5 Density of the Cloud

Density of mixture at constant temperature can be calculated from the equation (3.10);

$$\rho = \frac{(M_a + M_g)}{\frac{M_a}{\rho_a} + \frac{M_g}{\rho_g}} \quad (3.10)$$

Where;

M_a – Entrained mass of air

M_g – Mass of the toxic gas

ρ – Density of the mixture

3.6 Concentration Profile

Based on the assumption that the toxic mass has a Gaussian distribution, the concentration is given using equations (3.11), (3.12), (3.13) and (3.14) [12].

$$C(x, y, z, t) = \frac{M_g G(x, y, z, t)}{\sqrt{2\pi}^3 \sigma_y^2 \sigma_z} \quad (3.11)$$

And;

$$G(x, y, z, t) = \exp[-\{y^2 + (x - x(t))^2\} \frac{1}{2\sigma_y^2} - \frac{z^2}{2\sigma_z^2}] \quad (3.12)$$

$$\sigma_y = \frac{r}{2.14} \quad (3.13)$$

$$\sigma_z = \frac{h}{2.14} \quad (3.14)$$

Where;

$C(x,y,z,t)$ – Concentration of a point in Cartesian coordinate at time t

G – Function

σ_y – Standard deviation in lateral direction

σ_z – Standard deviation in vertical direction

$x(t)$ – position of the cloud center given by equation (3.15)

$$x(t) = ut \quad (3.15)$$

Where;

u – Wind velocity

t – Time

3.7 Model Equations

The basic equations in the model were summarized in Table 3.1. Constants are obtained through the best fit values obtained at model validation.

Table 3.1 Model Equations used in the simulation

Category	Eq No.	Equation	Constant	Assumption
Gravity Slumping	3.1	$V = \pi r^2 h$		$r = h$ at $t = 0$
	3.2	$\frac{dr}{dt} = U_f$		
	3.3	$\frac{dr}{dt} = C \sqrt{gh \frac{(\rho_g - \rho_a)}{\rho_g}}$	$C=1.3$	
Entrainment of air	3.4	$\frac{dM_a}{dt} = \rho_a(\pi r^2)U_e + 2\rho_a(\pi r h)\alpha^*(dr/dt)$	$\alpha^* = 0.5$	
	3.5	$U_e = \alpha' U_l R_i^{-1}$	$\alpha' = 0.6$	
	3.6	$R_i = \left(\frac{g l_s}{U_l^2}\right) \Delta\rho/\rho_g$		$\frac{U_l}{U_*} = 1.6$
	3.7	$l_s = 5.88h^{0.48}$		
Post transition period	3.8	$r = r_T + 2U_*(t - t_T)$		
	3.9	$h = r_T + \alpha'' U_*(t - t_T)$	$\alpha'' = 0.5$	$\frac{U_*}{U} = 0.1$
Cloud Density	3.10	$\rho = \frac{(M_a + M_g)}{\frac{M_a}{\rho_a} + \frac{M_g}{\rho_g}}$		
Concentration within volume	3.11	$C(x, y, z, t) = \frac{M_g G(x, y, z, t)}{\sqrt{2\pi^2 \sigma_y^2 \sigma_z^2}}$		Gaussian distribution
	3.12	$G(x, y, z, t) = \exp[-\{y^2 + (x - x(t))^2\}/2\sigma_y^2 - z^2/2\sigma_z^2]$		
	3.13	$\sigma_y = r/2.14$		
	3.14	$\sigma_z = h/2.14$		
	3.15	$x(t) = ut$		

3.8 Numerical Simulation of Model Equations

Numerical methods were used to solve the differential equations in the model. For ease of solving, mathematical software MATLAB was used. MATLAB is a mathematical software, originated and mainly developed by mathematicians [13].

A set of tools are provided in this mathematical software for solving model equations both analytically and numerically. The risk of programming errors was minimized by the use of these tools.

3.9 Case Study of Heavy Gas Release

As per the available data from Sri Lanka Customs one of the major chemicals imported that can be fallen into the heavy gas category is Chlorine, where 1666559 kgs were imported in 2011 and 1870418 kgs were imported in 2012 [14]. Therefore, for the present study Chlorine is selected as the heavy gas to simulate the model formulated in this work. The dispersion of this negatively buoyant and highly toxic gas is used to illustrate the use of dispersion modeling for risk and hazard analysis studies.

In 2012 there was an accident where gas pipeline connected to a chlorine tank exploded in a factory at the Kalutara Industrial Zone, leaving 11 people including three employees injured [4]. Therefore, in this study the location at Kalutara Industrial Zone was considered for the application of this model.

Chlorine gas imported in 900kg capacity cylinders have been used to refill into 68kg capacity cylinders in the Refilling Unit located in Fullertan Industrial Estate, Kalutara [15]. As 900 kg capacity cylinders are used in industrial applications, in this heavy gas dispersion model, the consequences of possible accidental release of the total containment in one 900kg cylinder of chlorine was examined.

3.9.1 Properties of Chlorine gas

Properties of Chlorine needed in the modeling study are illustrated in Table 3.2.

Table 3.2 Properties of chlorine

Atomic Number	17
Atomic Weight	35.457
1st Ionization Energy	1251 kJ/mol
Density (Dry Gas)	3.214 g/L
Melting Point	-101°C

A Chlorine spill into atmospheric conditions from a pressurized tank will boil and vaporize rapidly, and a denser-than-air gas cloud will be formed. Since the released dense gas is toxic, the data regarding both the concentration levels and the time variation to estimate the effects of exposure had become important.

Chlorine is regarded as an irritant gas and the most serious effect of acute chlorine poisoning damages the respiratory system. Effects of chlorine on human health depend on the amount of chlorine that is present, and the length and frequency of exposure. Effects also depend on the health of a person or condition of the environment when exposure occurs.

Information on the toxicity of chlorine was studied by Dicken and the relationship between toxicity and time of exposure is shown in below Figure 3.2 [11].

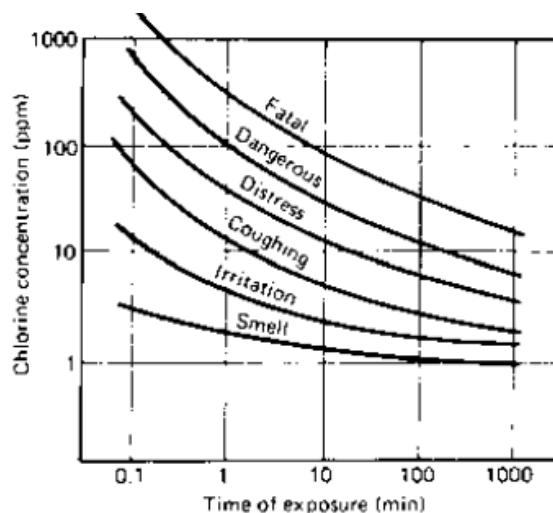


Figure 3.2 Effects of exposure to different concentrations of chlorine

Below Table 3.3 represents the concentrations of chlorine levels with tolerance limit [11].

Table 3.3 The concentrations of chlorine tolerable and intolerable to man

Author(s)	Effect	Conc. (ppm)	Exposure time (h)
Rupp and Henschler (1967)	Odour threshold	0.02 - 0.05	
ACGIH	Threshold limit value	1	
Kobert (1912)	Minimum concentration to detect odour	3.5	
	Concentration which causes immediate irritation	14	
	Concentration which causes coughing	28	
	Dangerous concentration	40	
Flury and Zernick (1931)	Concentration tolerable without immediate or later consequences	3.5	0.5 – 1
	Concentration at which work can be continued without interference	1-2	
	Concentration at which work becomes impossible	4	
	Dangerous concentration	14 - 21	0.5 – 1
Henderson and Haggard (1943)	Maximum concentration allowable for physical exertion	0.35 - 1	
	Minimum concentration to detect odour	3.5	
	Maximum concentration allowable for short exposure	4	0.5 – 1
	Dangerous concentration for short exposure	40 - 60	
Vedder (1941)	Concentration which incapacitates man (crying, coughing) in a few seconds	100	
Wachtel (1941)	Concentration which causes severe irritation	3	
	Concentration which causes loss of fighting capacity	47	
Patty (1962)	Concentration which causes irritation	3-6	
	Intolerable concentration	100	

3.9.2 Input data to the model

When developing the model much information is needed to be gathered since the atmospheric dispersion of toxic materials is affected by a wide variety of parameters. Any uncertainties and errors in these inputs will be reflected in the model results, so this step is critical to the quality of the dispersion modeling effort.

3.9.2.1 Meteorological data

The meteorological data used in the dispersion model was considered to be important since the transport and dispersion of the emissions in the atmosphere was driven by that. The application of this model was done to a release scenario in Kaluthara district hence the meteorological data in Kaluthara district was considered.

➤ Wind speed

The mean monthly wind speed over the year 2015 in Kalutara was ranged from 1.5 m/s to 2.3 m/s at 10m height [16].

➤ Atmospheric stability class

This indicates the dispersive ability of the atmosphere relating to vertical mixing of the air. The concept of atmospheric stability is very important for the evaluation of supporting capacity of the atmosphere and is used extensively in dispersion modeling. Pasquill stability criteria was used for identifying the atmospheric stability class, in which atmospheric stability is classified according to six stability classes: named A, B, C, D, E and F with class A being the most unstable or most turbulent class, and class F the most stable or least turbulent class [11]. The six stability classes with definitions are given in Table 3.4 [17].

Table 3.4 Pasquill stability classes

Stability class	Definition	Stability class	Definition
A	Very unstable	D	Neutral
B	Unstable	E	Slightly stable
C	Slightly unstable	F	Stable

Surface wind speed, intensity of solar radiation and night time sky cover are the prime factors defining the atmospheric stability classes which is illustrated in Table 3.5 [17].

Table 3.5 Meteorological conditions affecting atmospheric stability class

Surface wind speed		Daytime incoming solar radiation			Night time cloud cover	
m/s	mi/h	Strong	Moderate	Slight	>50%	<50%
<2	<5	A	A-B	B	E	F
2-3	5-7	A-B	B	C	E	F
3-5	7-11	B	B-C	C	D	E
5-6	11-13	C	C-D	D	D	D
>6	>13	C	D	D	D	D

Since in Kalutara area, wind speed is varied from 1.5 to 2.3 m/s and has a moderate incoming solar radiation [16], stability class “A” was adopted in the present study suggesting a wind velocity of 1.5 m/s for predicting the “worst scenarios” in the area.

➤ Ambient temperature

For impact assessments, the maximum and minimum ambient temperatures that are representative of the site must be included in the meteorological data. In Kalutara area the maximum and minimum temperature varies from 32 °C to 22 °C, and these values were considered in the model [16].

3.9.2.2 Release height

The release height significantly affects ground-level concentrations. As the release height increases, ground-level concentrations are reduced because the gas cloud must disperse a greater distance vertically.

In the present study heavy gas release from a catastrophic failure of a pressurized tank located on the ground was considered. Hence the height of release was taken to be at ground level.

3.9.2.3 Terrain and sensitive receptors

The dispersion modeling input requires information regarding the surrounding terrain and sensitive receptors. Terrain and receptor are which include the location and height in meters relative to a fixed origin. The location of any particularly sensitive receptors (and likely future sensitive receptors) such as residences, schools and hospitals can also be specifically included.

3.9.2.4 Building wake effects

The location and dimensions of buildings located within a distance of $5L$ (where L is the lesser of the height or width of the building) should be considered. For dense gases flowing over surfaces where the topographical features are large enough to be an actual obstruction to the flow it might behave as if it is encountering an inclination or it might be confined by the obstacle.

The input data used in the model are summarized in Table 3.6.

Table 3.6 Input data used in the model

Parameter	Data
Wind Speed (U)	1.5 m/s
Atmospheric stability class	A
Ambient temperature	22-32°C
Mixing height	Ground level
U^*/U value for open terrain	0.1

3.10 Calculation

Using the collected data, the model calculations were proceeded in the following manner.

3.10.1 Gravity slumping phase

At initial conditions (t=0);

$$M_g = 900 \text{ kg}$$

$$C = 1.3;$$

$$\rho_g = 3.214 \text{ kg/m}^3$$

$$\rho_a = 1.225 \text{ kg/m}^3$$

$$g = 9.8 \text{ m/s}^2$$

From equation (3.3) in Table 3.1,

$$\frac{dr}{dt} = C \sqrt{gh \frac{(\rho_g - \rho_a)}{\rho_g}}$$

$$\frac{dr}{dt} = 1.3 \sqrt{9.8 \text{ m/s}^2 \times h \frac{(3.214 \text{ kg/m}^3 - 1.225 \text{ kg/m}^3)}{3.214 \text{ kg/m}^3}}$$

$$\frac{dr}{dt} = 3.2\sqrt{h}$$

$$\frac{dr}{dt} = 3.2\sqrt{h} \text{----- (A)}$$

Volume (V_0) and density are constants for no entrainment of air at initial point.

Therefore, V_0 is calculated as:

$$V_0 = \frac{M_g}{\rho_g}$$

$$V_0 = \frac{900 \text{ kg}}{3.214 \text{ kg/m}^3}$$

$$V_0 = 280 \text{ m}^3$$

By equation (3.1) in Table 3.1 volume of the cylinder, V;

$$V = \pi r^2 h$$

At t=0, $r_0 = h_0$;

$$V_0 = \pi r_0^2 h_0$$

$$280 \text{ m}^3 = \pi r_0^3$$

$$280 \text{ m}^3 = \pi r_0^3$$

$$r_0 = h_0 = 4.466 \text{ m}$$

Where;

r_0 - initial radius of cloud at $t = 0$

h_0 - initial height of cloud at $t = 0$

From (3.1) and (A);

$$\frac{dr}{dt} = 3.2\sqrt{h}$$

3.10.2 Air entrainment phase

The entrained mass equation is given by equation (3.4) in Table 3.1;

$$\frac{dM_a}{dt} = \rho_a(\pi r^2)U_e + 2\rho_a(\pi r h)\alpha^*(dr/dt)$$

Top entrainment velocity U_e is given by equation (3.5) in Table 3.1;

$$U_e = \alpha' U_1 R_i^{-1}$$

Above equation is valid when $U_e \leq U_1$. Here U_1 is the longitudinal turbulence velocity which is proportional to the friction velocity U^* .

The ratio values of (U_1/U^*) has been shown by Monin primarily based on the stability condition [11]. The constant of proportionality (U_1/U^*) being 1.6 for very unstable and category A-B weather, 2.4 for neutral and category C-D weather or 3 for very stable and category E-F weather [11].

Hence for the atmospheric conditions in this study, $U_1/U^* = 1.6$

The ratio (U^*/U) has been shown by O.G. Scutton primarily based on the surface roughness. A typical value for open terrain is 0.1 [11].

$$U^*/U = 0.1$$

$$\begin{aligned} \text{Hence, } (U_1/U) &= (U_1/U^*) \times (U^*/U) \\ &= 1.6 \times 0.1 \\ &= 0.16 \end{aligned}$$

$$\begin{aligned} \text{Therefore } U_1 &= 0.16 \times U \\ &= 0.16 \times 1.5 \text{ m/s} \\ &= 0.24 \text{ m/s} \end{aligned}$$

To calculate the top entrainment velocity, Richardson number and turbulence length scale has to be considered in equation (3.6) and (3.7) in Table 3.1.

$$R_i = \left(\frac{g l_s}{U_1^2} \right) \frac{(\rho_g - \rho_a)}{\rho_g}$$

Turbulence length scale;

$$l_s = 5.88 h^{0.48}$$

$$\frac{dM_a}{dt} = \rho_a (\pi r^2) U_e + 2 \rho_a (\pi r h) \alpha^* (dr/dt)$$

Substituting equation (3.5);

$$\frac{dM_a}{dt} = \rho_a (\pi r^2) \alpha' U_1 / R_i + 2 \rho_a (\pi r h) \alpha^* (dr/dt)$$

Substituting equation (3.6);

$$\frac{dM_a}{dt} = \rho_a(\pi r^2)\alpha' U_l / \left(\frac{gl_s}{U_l^2} \right) \Delta\rho + 2\rho_a(\pi r h)\alpha^*(dr/dt)$$

$$\frac{dM_a}{dt} = \rho_a(\pi r^2)\alpha' U_l^3 / \left(\frac{gl_s}{\rho_g} \right) \Delta\rho + 2\rho_a(\pi r h)\alpha^*(dr/dt)$$

$$\frac{dM_a}{dt} = \rho_a \rho_g (\pi r^2)\alpha' U_l^3 / gl_s \Delta\rho + 2\rho_a(\pi r h)\alpha^*(dr/dt)$$

Substituting equation (3.7);

$$\frac{dM_a}{dt} = \rho_a \rho_g (\pi r^2)\alpha' U_l^3 / g 5.88 h^{0.48} \Delta\rho + 2\rho_a(\pi r h)\alpha^*(dr/dt)$$

$$\frac{dM_a}{dt} = 0.000894202 r^2 / h^{0.48} + 3.848451001 r h (dr/dt) \text{-----(B)}$$

Substituting equation (A);

$$\frac{dM_a}{dt} = 0.000894202 r^2 / h^{0.48} + 12.32702489 r h^{1.5}$$

From Equation (3.1);

$$V = \pi r^2 h$$

$$M/\rho = \pi r^2 h$$

$$\frac{M_a}{\rho_a} + \frac{M_g}{\rho_g} = \pi r^2 h$$

Differentiating by t,

$$\frac{d}{dt} \left(\frac{M_a}{\rho_a} + \frac{M_g}{\rho_g} \right) = \frac{d}{dt} (\pi r^2 h)$$

$$\frac{1}{\rho_a} \frac{dM_a}{dt} = \pi r^2 \left(\frac{dh}{dt} \right) + 2\pi r h \left(\frac{dr}{dt} \right)$$

$$\frac{dM_a}{dt} = \rho_a \pi r^2 \left(\frac{dh}{dt}\right) + 2\rho_a \pi r h \left(\frac{dr}{dt}\right)$$

$$\frac{dM_a}{dt} = 3.848451001r^2 \left(\frac{dh}{dt}\right) + 7.696902001rh \left(\frac{dr}{dt}\right) \text{-----(C)}$$

By equating (B) and (C);

$$\begin{aligned} \frac{0.000894202r^2}{h^{0.48}} + 3.848451001rh \left(\frac{dr}{dt}\right) \\ = 3.848451001r^2 \left(\frac{dh}{dt}\right) + 7.696902001rh \left(\frac{dr}{dt}\right) \end{aligned}$$

$$\begin{aligned} 3.848451001r^2 \left(\frac{dh}{dt}\right) \\ = \frac{0.000894202r^2}{h^{0.48}} + 3.848451001rh \left(\frac{dr}{dt}\right) - 7.696902001rh \left(\frac{dr}{dt}\right) \end{aligned}$$

$$3.848451001r^2 \left(\frac{dh}{dt}\right) = \frac{0.000894202r^2}{h^{0.48}} - 3.848451001rh \left(\frac{dr}{dt}\right)$$

$$\left(\frac{dh}{dt}\right) = \frac{0.000232354}{h^{0.48}} - 3.203113378h^{1.5}/r$$

Now we can solve the following three equations by ODE solver in Matlab;

$$\frac{dr}{dt} = 3.2\sqrt{h}$$

$$\frac{dh}{dt} = \frac{0.000232354}{h^{0.48}} - 3.203113378h^{1.5}/r$$

$$\frac{dM_a}{dt} = 0.000894202r^2/h^{0.48} + 12.32702489rh^{1.5}$$

3.10.3 Post transition phase

When $\rho_g - \rho_a < 0.001 \text{ kgm}^{-3}$, it is assumed that the plume becomes passive [18]. The radius and height can be calculated by equation (3.8) and (3.9) in Table 3.1.

$$r = r_T + 2U_*(t - t_T)$$

$$h = h_T + \alpha U_*(t - t_T)$$

Relevant matlab m files are attached in Appendix A-F.

3.11 Numerical Simulation

Ordinary Differential Equation (ODE) solver in Matlab was used to solve the differential equations of heavy gas cloud dispersion behavior and to obtain the relationship between the cloud shape characteristics with time. (The relevant matlab m files developed to solve these equations are shown in Appendix A to F). The relationship between the cloud shape characteristics with time, the relationship between the quantity of air entrainment and the time from release and predicted maximum concentration at various downwind distances on the ground level from the release point were obtained.

3.12 Model Validation

In order for the model results to be relied upon, the model should be validated to demonstrate that the model can produce reliable results for a given modeling scenario. This validation process allows the model performance to be assessed and verified and brings confidence in the model results for scenarios under which validation of the model has occurred.

Therefore the comparison of model predictions with appropriate field experiment results was done to assess the performance of the model. Therefore, the present

model was validated by considering the experimental results of Thorney Island field trials done using Freon+N₂ for an instantaneous release.

The heavy gas dispersion trials at Thorney Island (U.K.) had been undertaken by the Health and Safety Executive (HSE) during years 1982-1984 [19]. The main trials had been carried out with instantaneous releases and conducted in two series, Phase I and Phase II. Phase I involved unobstructed releases over a flat surface. Phase II releases over a flat surface with obstructions. In this work phase I results were considered in validation of the model. The phase one trials involved an instantaneous release of 2000m³ of a heavy gas-nitrogen mixture. The gas used was Feron 12, the proportion being varied to give mixtures of different relative density up to 4.2 [11]. The aim of the Phase I trials had been to obtain data which could be used to validate models. This phase had included sixteen trials obtaining plenty of test data.

A former Royal Air Force station at Thorney Island had been used as the site to carry out the above trials by HSE. The test area had included a length of 2 km and a width of 500 m and flat to within 1 in 100 [23]. The expected wind speeds in the site had been in the range 1.5 m/s to 9 m/s [20]. The details of the ground conditions of this trial site including spill point, permanent buildings and grasslands are available in the work published by HSE [20].

In the present study, the model was validated using Trial number 008 experimental data. These experimental data are given in Table 3.7 [20]. The predicted maximum ground level centerline gas concentrations from present work model compared with the maximum observed concentrations from Thorney Island trial as a function of downwind distance from the release center are given in Table 3.8 [19].

Table 3.7 Experimental data in Thorney Island Trial 008

Date and time of release	9 September 1982, 17:49:58 hrs
Initial relative density ratio	1.63
Initial cloud volume	2000 m ³
Mean wind speed	2.4 m/s
Mean wind heading	-15.8°
Relative humidity	87.6%
Insolation	158 W/m ²
Treated runway surface temperature	18.4°C
Ambient air temperature	17.12°C
Grass surface temperature	18.4°C
Observed cloud cover	2/8
Stability condition	D

Source: (J. McQuaid and B. Roebuck, *Large scale field trials on dense vapour dispersion* [20].)

Table 3.8 Observed and predicted maximum concentrations at various downwind distances in Thorney Island Trial 008

Downwind Distance (m)	Observed * Concentration (mol%)	Predicted (model) Concentration (mol%)	Error %
71	9.25	6.74	-37.33
100	6.11	5.92	-3.28
150	4.03	4.28	5.95
200	2.81	2.94	4.35
364	1.08	1.03	-5.32
412	0.69	0.79	12.17
510	0.43	0.48	10.30

* Source: (M. Mohan, T. Panwar and M. Singh, *Development of dense gas dispersion model for emergency preparedness [19]*)

From the calculated error percentages in Table 3.8, the comparison could be considered as fairly good with most of the data points being in close agreement to the observed values. This is further illustrated in Figure 3.3.

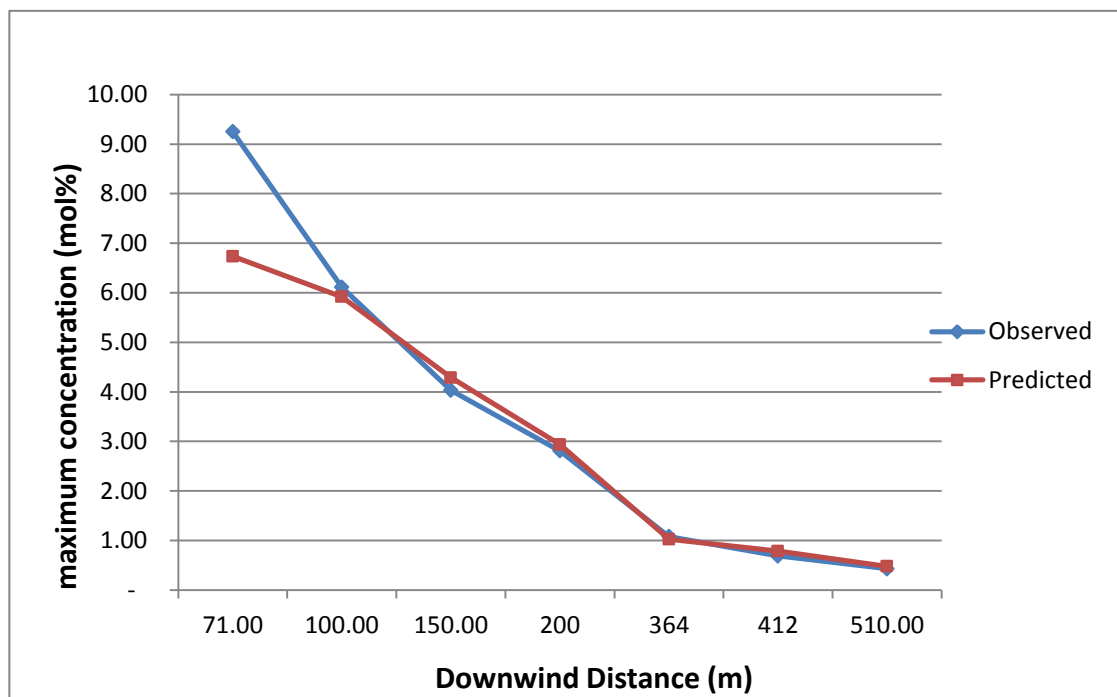


Figure 3.3 Model validation data points

Since predicted model downwind concentrations are in consistent with the data from the field tests, model is considered as properly validated. (Model validation and sensitivity analysis of parameters is in Appendix H.)

3.13 Interpretation of Dispersion Modeling Results

The simulated results are used for the risk assessment using probit function and determining the harmful concentration levels.

Probit equation given by Eisenberg, Lynch and Breeding for lethality is considered in the analysis, which is given by the following relation [11]:

$$Y = -17.1 + 1.69\ln(\Sigma C^{2.75}t) \quad (3.16)$$

This relationship applied to healthy adults and susceptible individuals such as infants, elderly people and people with advanced pulmonary/cardiovascular disease.

To determine the harmful chlorine concentration levels, IDLH value of 30 ppm was considered which represents the maximum concentration from which, in the event of respiratory failure, one could escape in 30 minutes without a respirator and without irreversible health effect [12]. The IDLH value was taken because it is more suitable for use as a workplace risk management tool and also in all cases it does describe a lower limit for survivability.

4 RESULTS AND DISCUSSION

The heavy gas model formulated in this work was used to simulate the dispersion of negatively buoyant and highly toxic chlorine to illustrate the use of dispersion modeling for risk and hazard analysis studies.

Considering a past release scenario occurred in Sri Lanka, the heavy gas model was used to evaluate the consequences. At the time of the incident, the site has handled 300 numbers of 900kg chlorine cylinders which had been stored for refilling into 68kg cylinders. A layout of the site is given in Figure 4.1. Therefore accidental release of a total containment in one 900kg cylinder of chlorine was examined using the heavy gas dispersion model and discussed in the following section.

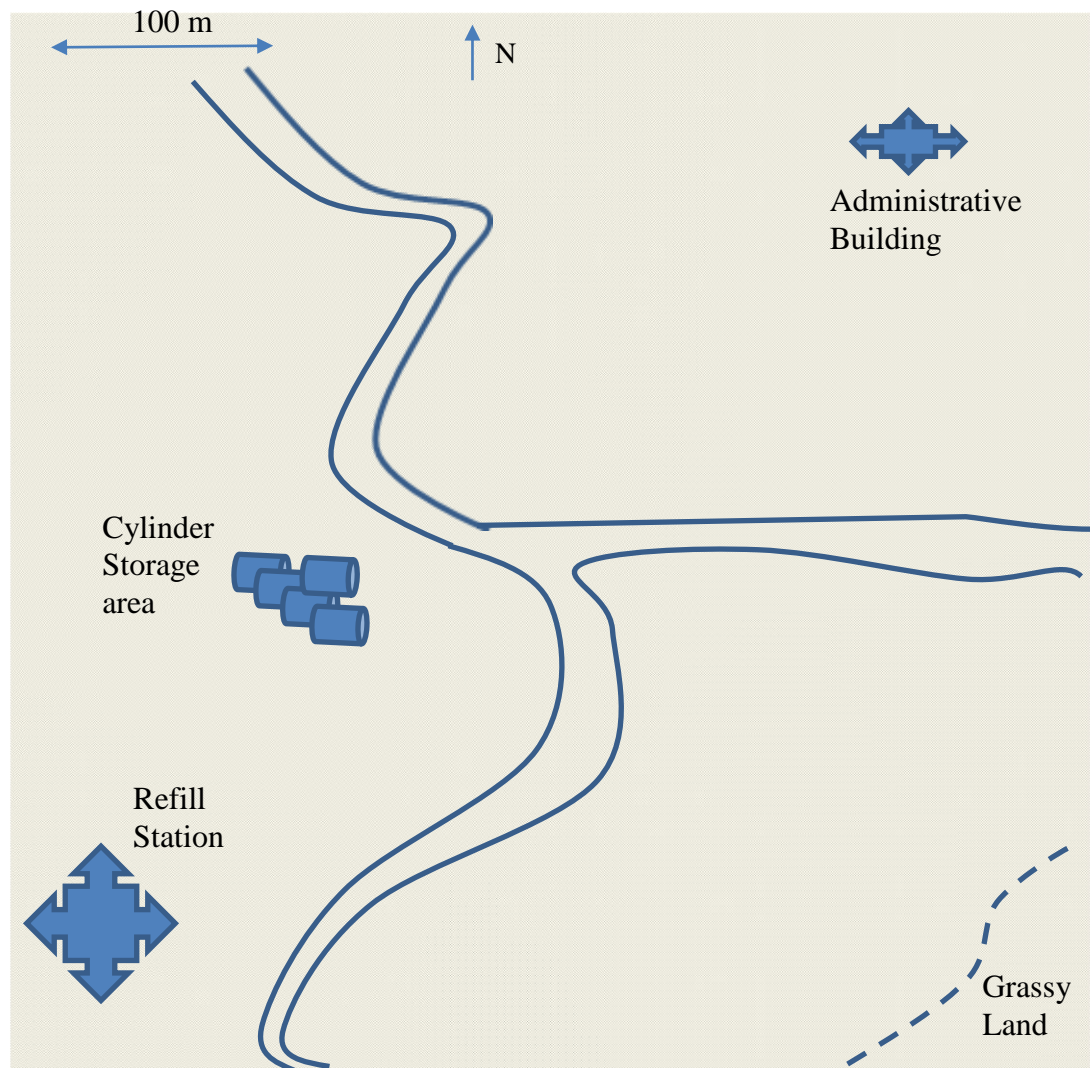


Figure 4.1 Site layout of the case study

4.1 Numerical Simulation Results

Numerical solution of the equations was used to estimate the cloud characteristics that are radius, height, density and amount of air entrained at each time step. The assumption in this model was that the initial stages of dispersion can be described by a modified box model and the atmospheric dispersion stage is described using a modified Gaussian, volume source based model. The predicted concentration values from the model can be used to identify hazardous zones which can be identified by calculating the safe downwind distances and critical time intervals.

4.2 Radius and Height Variation with Time

4.2.1 Gravity slumping phase

In this primary phase, the density difference between the cloud and the ambient air results in gravitational slumping. Therefore cloud radius increases and cloud height decreases quickly because of effect of turbulence resulted from gravitational slumping.

In Figure 4.2 this is illustrated, where the rate of change of cloud radius decreases gradually. At the initial point radius of the cylinder is calculated as 4.5 m which is the same as the initial cloud height. Since the vapor cloud is heavier than air (negatively buoyant), cloud will eventually lie at the ground level after being released.

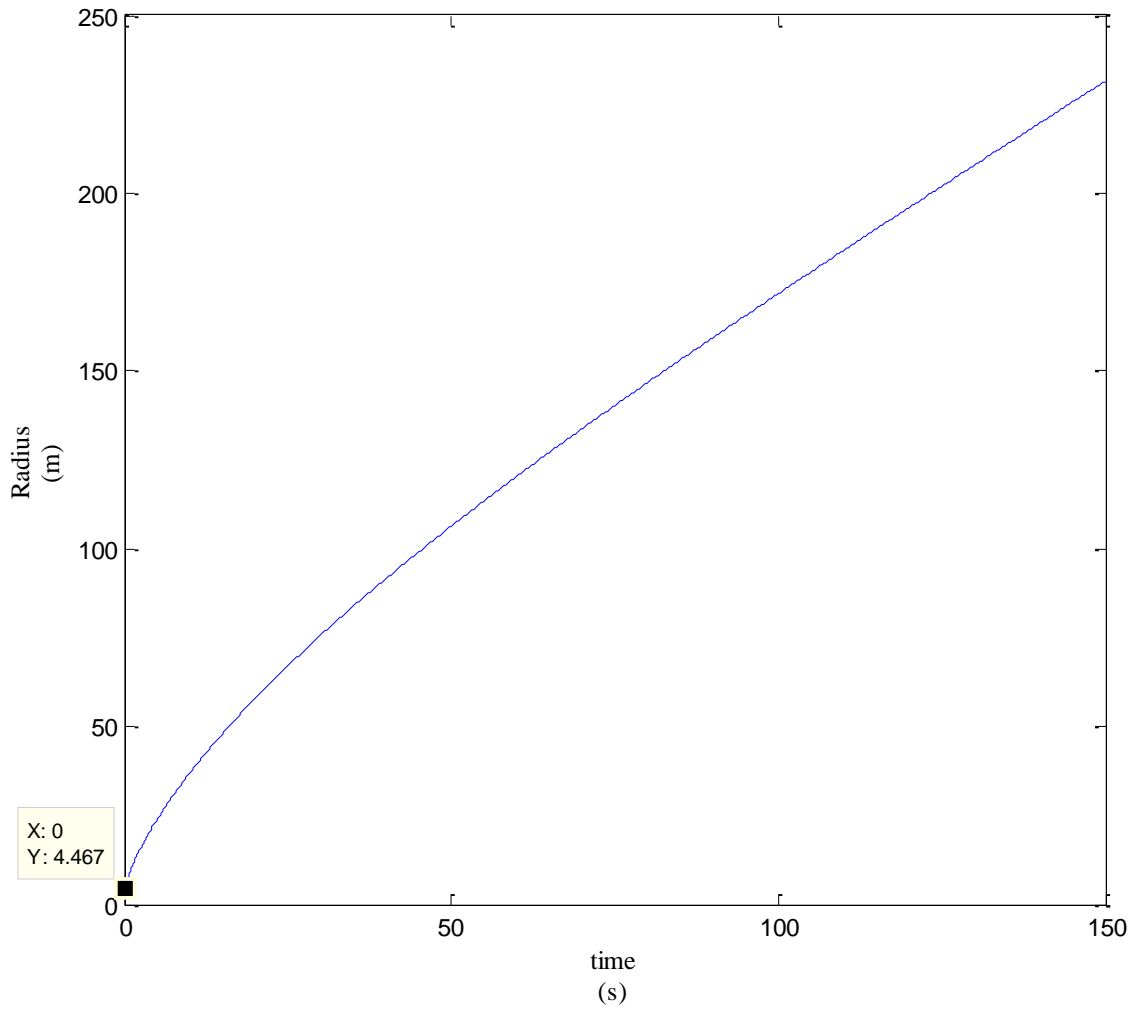


Figure 4.2 Variation of cloud radius with time during gravity slumping phase

During this gravity slumping phase, cloud height decreases at a higher rate in first 10 seconds and then the rate of change decreases as illustrated in Figure 4.3.

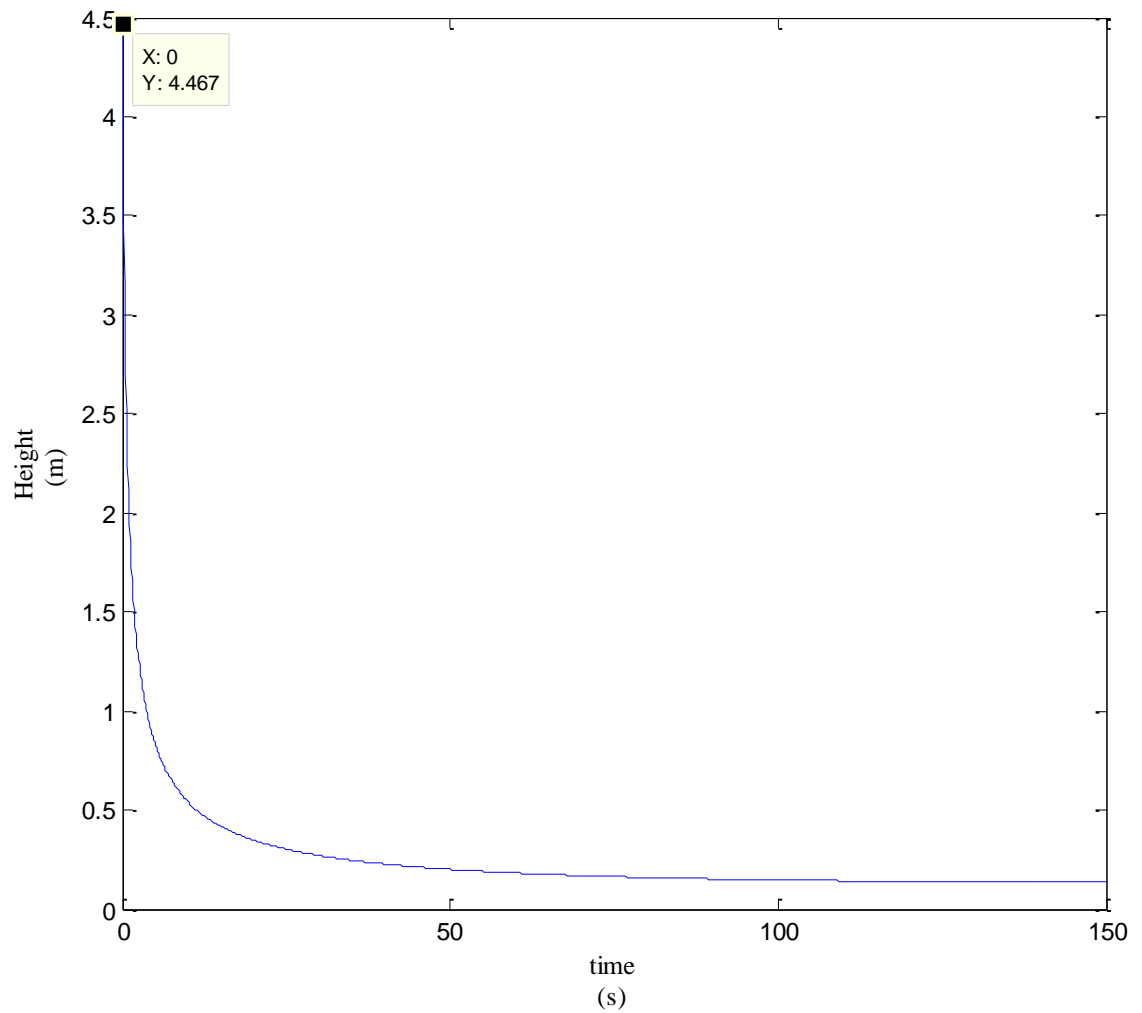


Figure 4.3 Variation of cloud height with time during gravity slumping phase

4.2.2 Air entrainment phase

At the air entrainment phase, heavy gas cloud dilutes and more air entrains which will affect the radius and height variation of the cloud. As quantities of air are entrained into the cloud, cloud density decreases and the cloud dispersion is dominated by atmospheric turbulence.

According to the graphs the transition from gravity spread to air entrainment occurs at the point where $h = 0.1342\text{m}$ and $t = 180\text{ s}$ (at the point where height is minimum). At that time $r = 266.7\text{ m}$ and $M_a = 36380\text{kg}$.

Then radius and height will further increase with time, which is illustrated in Figure 4.4 and Figure 4.5. This has caused further increase of the cloud volume which has resulted in a lower concentration value within the cloud. The increase in cloud volume is only caused by air entrainment so the toxic gas is diluted by the air volume in the cylinder, which will finally lead to the passive dispersion phase where gravity dominance is taken over by the atmospheric turbulence.

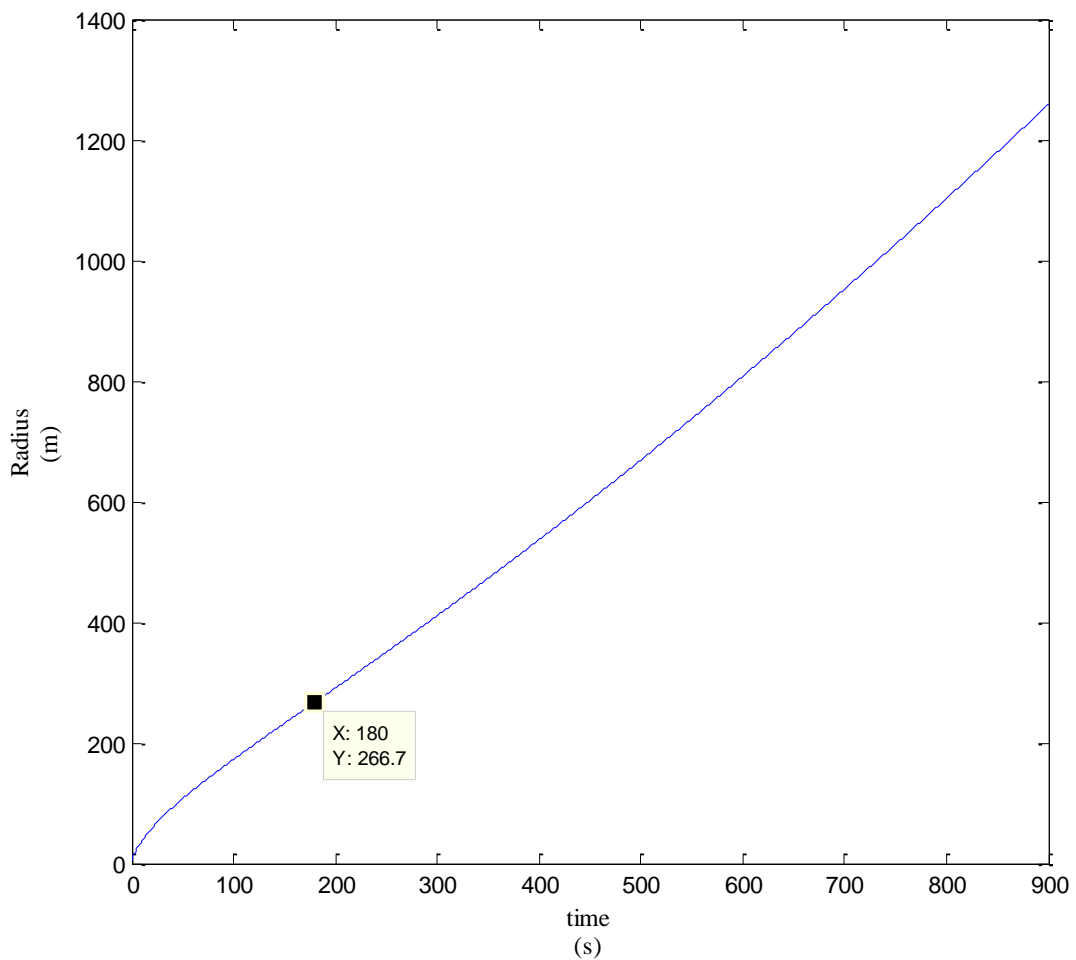


Figure 4.4 Variation of cloud radius with time during air entrainment phase

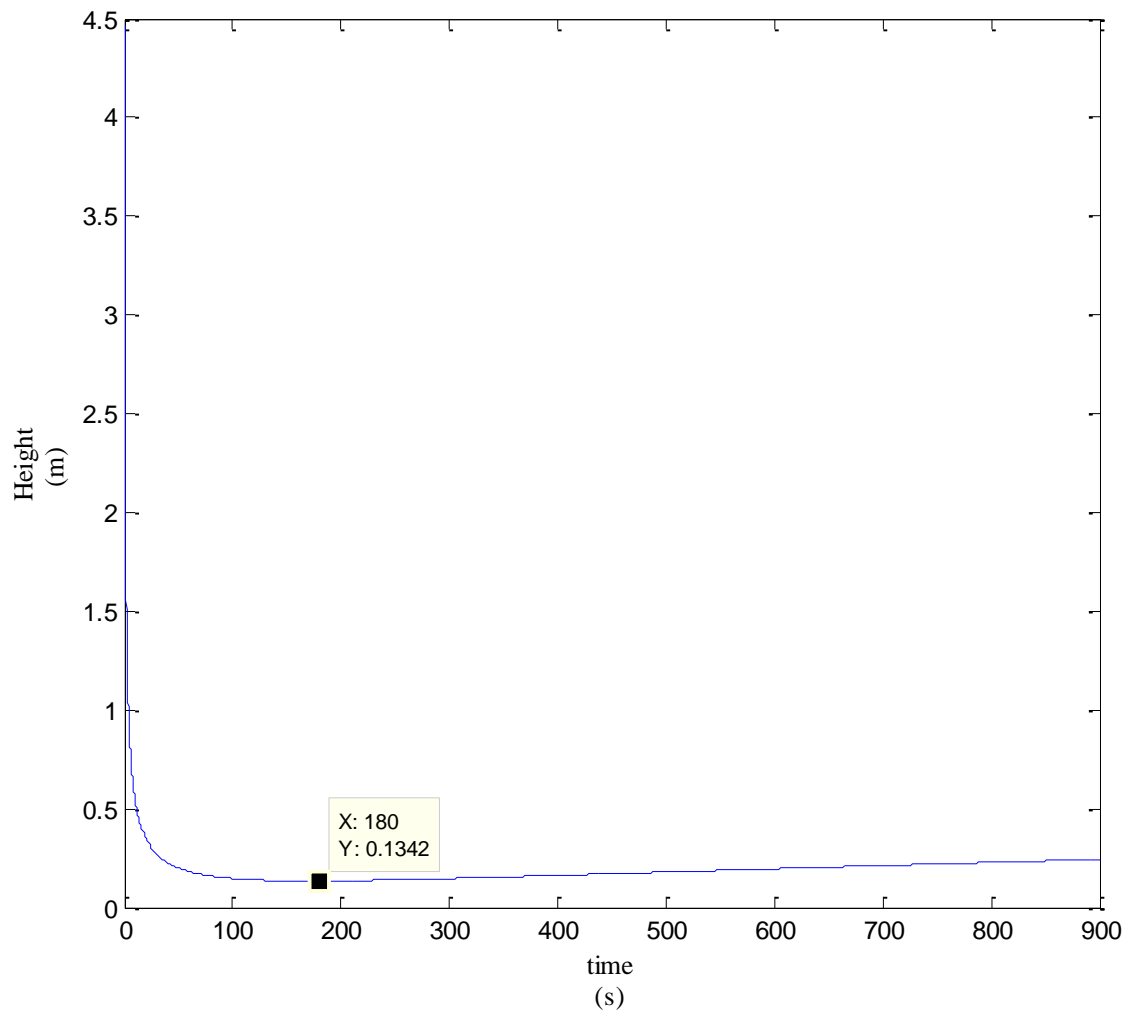


Figure 4.5 Variation of cloud height with time during air entrainment phase

The entrained air mass rate will gradually increase at the air entrainment phase as shown in figure 4.6.

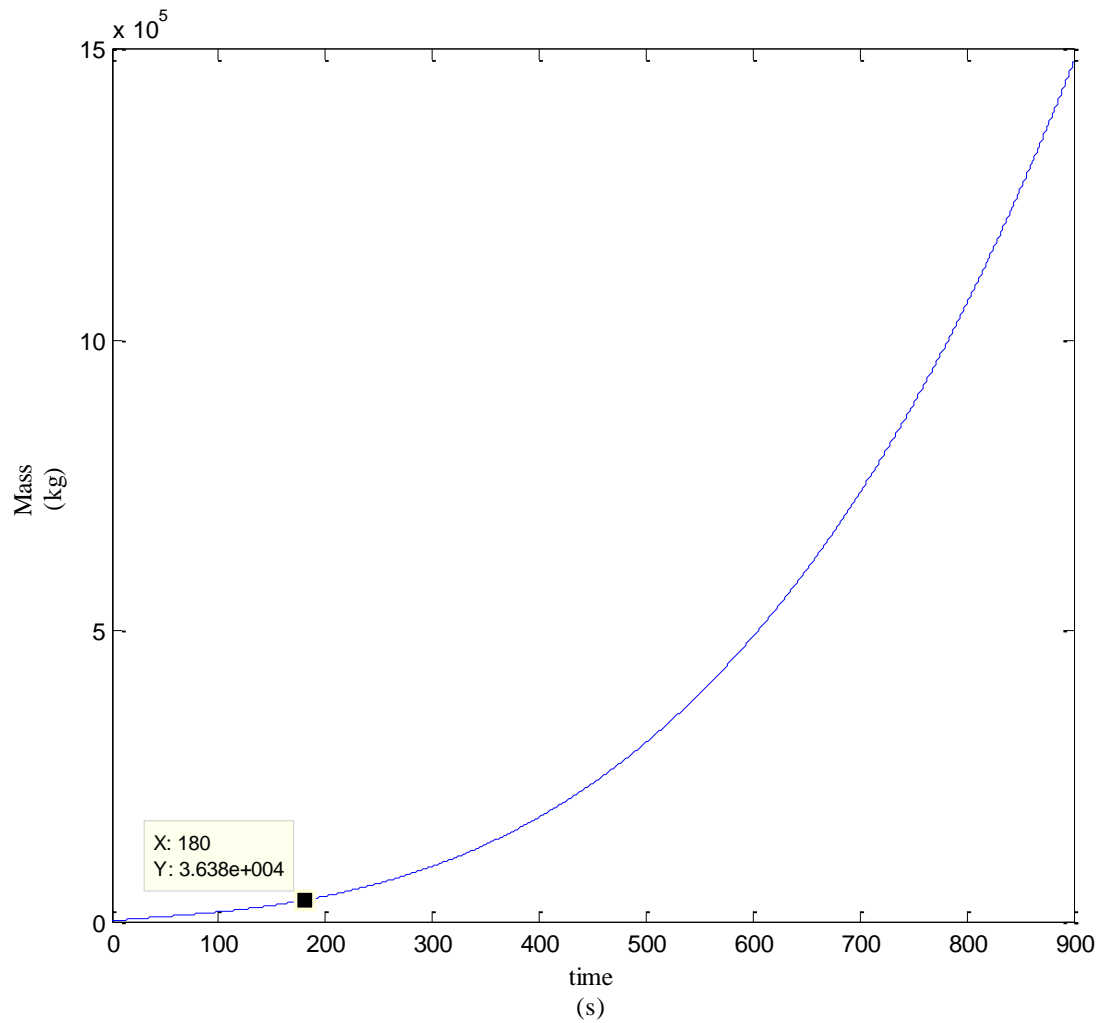


Figure 4.6 Variation of entrained air mass with time during air entrainment phase

In the heavy gas dispersion phase, the change rate of quantity of air increasing gradually indicates the special phenomena in heavy gas dispersion process. That is in first few seconds there is relatively little change in the cylinder volume. As $\Delta\rho/\rho_a \rightarrow 0$, the increase in cloud volume is only caused by entrainment so the rate of change of entrainment of air is higher and higher.

4.2.3 Post transition phase

When the density difference between air and cloud become negligible, i.e; $\rho_g - \rho_a < 0.001$, transition occurs to the passive dispersion phase [18]. According to the simulation results the transition to passive dispersion phase occurs around 680s from release. Then radius and height of the cloud increase with time in a linear manner, and air entrainment ceases, as shown in figure 4.7 and figure 4.8 respectively.

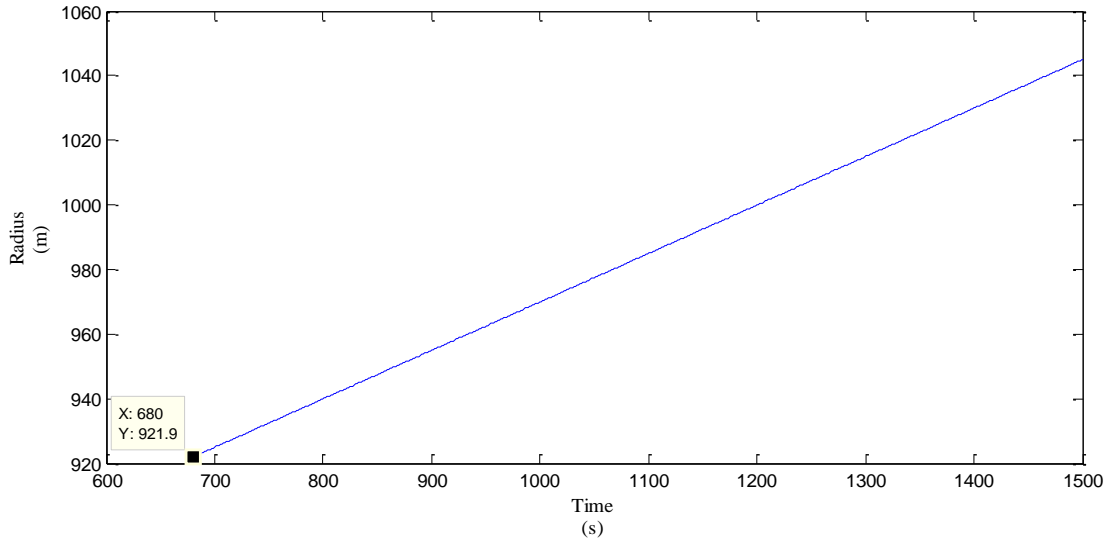


Figure 4.7 Variation of radius during post transition phase

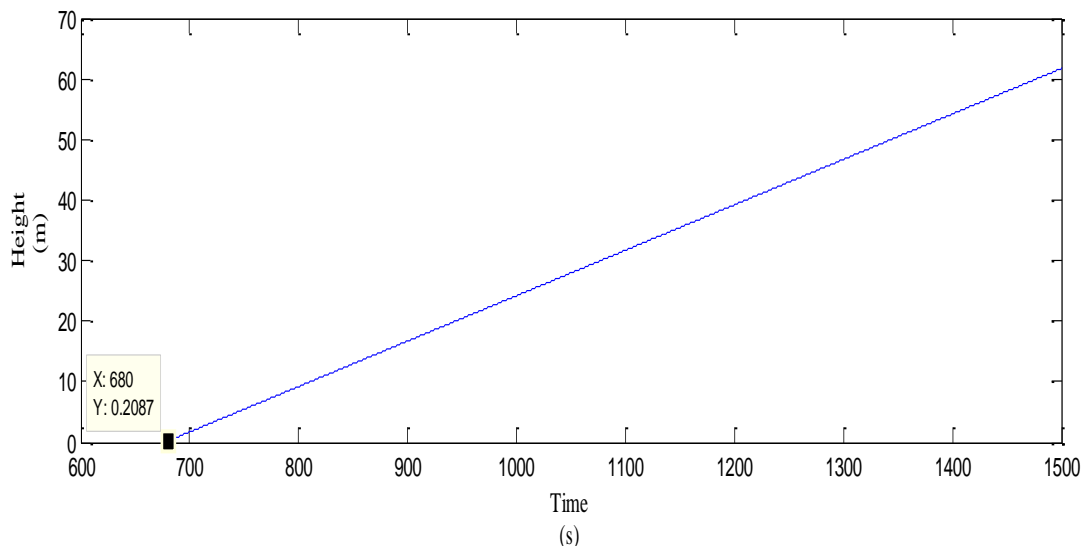


Figure 4.8 Variation of height during post transition phase

When all three phases are combined, the variation of radius and height with time are shown in Figure 4.9. From 0 to 180s gravity slumping phase prevails, then air entrainment phase dominates till 680s when the transition to the passive phase occurs after that.

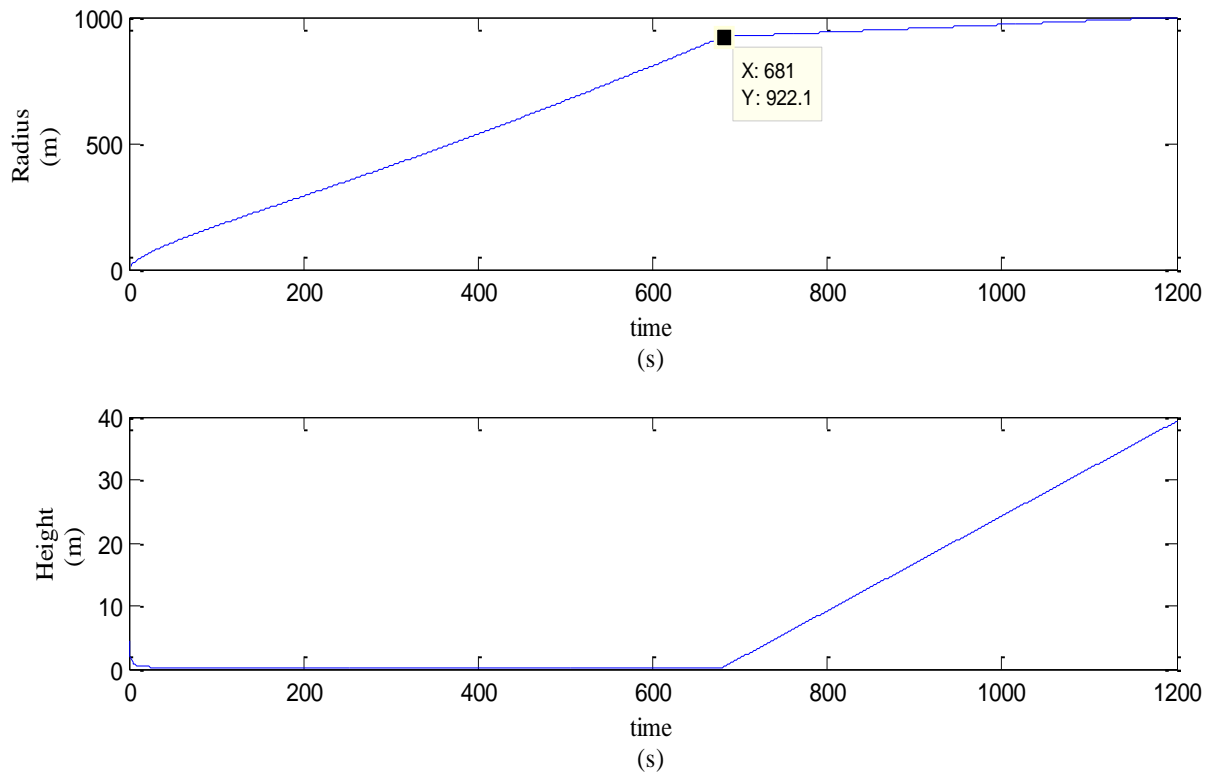


Figure 4.9 Variation of radius and height during all three phases

According to the above Figure 4.9 we can see that air entrainment occurs until the cloud radius becomes is 922m. Until that point the cloud height is below 1 m but when the passive dispersion occurs, height starts to increases at a constant rate. But when we look at this figure we can see that the transition point is not that smooth. Hence transition criteria used i.e; the density difference between air and cloud is less than 0.001kg/m^3 [18], can be further studied to obtain the optimum value. But at this point the concentration levels in the gas cloud are minimized to be lower than the harmful values; hence this will not exercise much impact.

4.3 Concentration Profile

The chlorine concentration at the cylindrical volume is remained high until sufficient air has diffused into the central regions. In fact, it was assumed that no reaction occurs after the transition from the heavy gas dominated dispersion to the atmospheric dominated dispersion.

The concentration at a given time varies along with the downwind distance. Initially it increases in downwind distance reaching a maximum value and then decreases. Figure 4.10 shows the concentration profile for 900kg release of chlorine as a function of downwind distance from 0 to 1000m, at times 50s, 100s and 150s after the release.

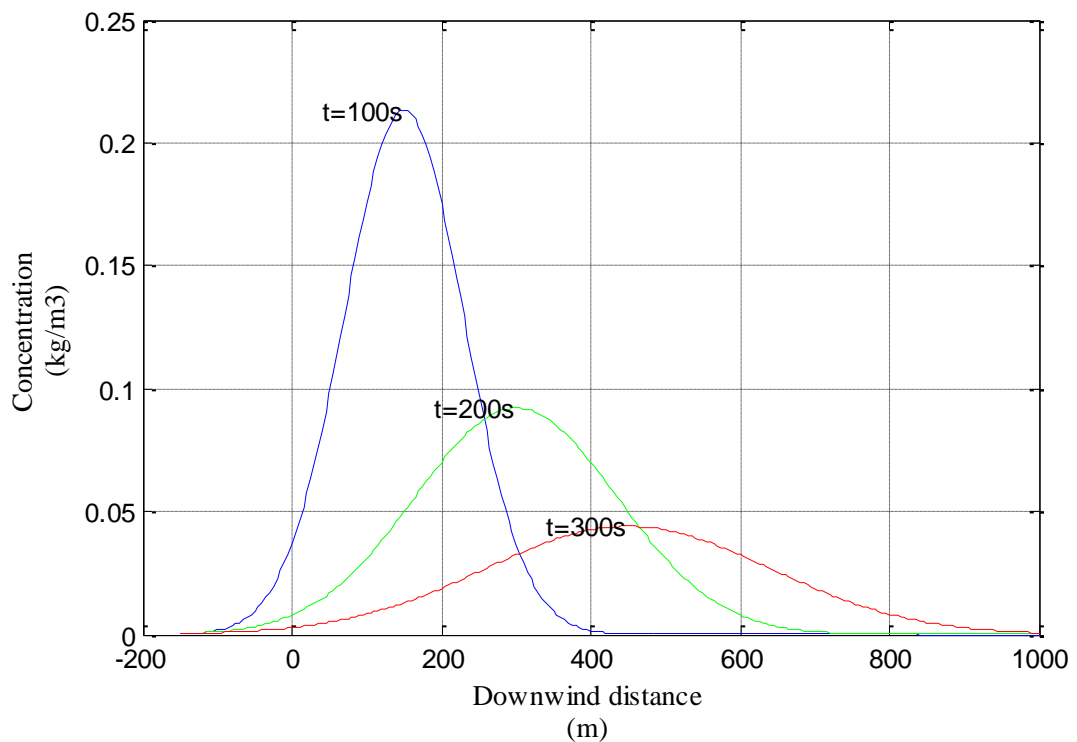


Figure 4.10 Concentration profile at different times after the release

The peak of the curves is the center of cloud which is having maximum concentration. At points away from the cloud center the concentration gets lower. The points of maximum concentration are 150m at 100s, 300m at 200s and 450m at 300s. At the time 100s after the release of chlorine the concentration value of chlorine is above the Immediately Dangerous to Life (IDLH) value which is

0.03kg/m^3 between distances 0m and 305m from the release point. For 200s it is above IDLH value between 105m and 495m and for 300s it is above IDLH value between 305m and 595m.

Assuming the toxic mass has a Gaussian distribution position of the cloud can be drawn on Cartesian coordinates at time t where (x,y,z,t) gives the position. This indicates how cloud moves in the down wind direction.

The propagation of contours in downwind direction is given in below Figure 4.11.

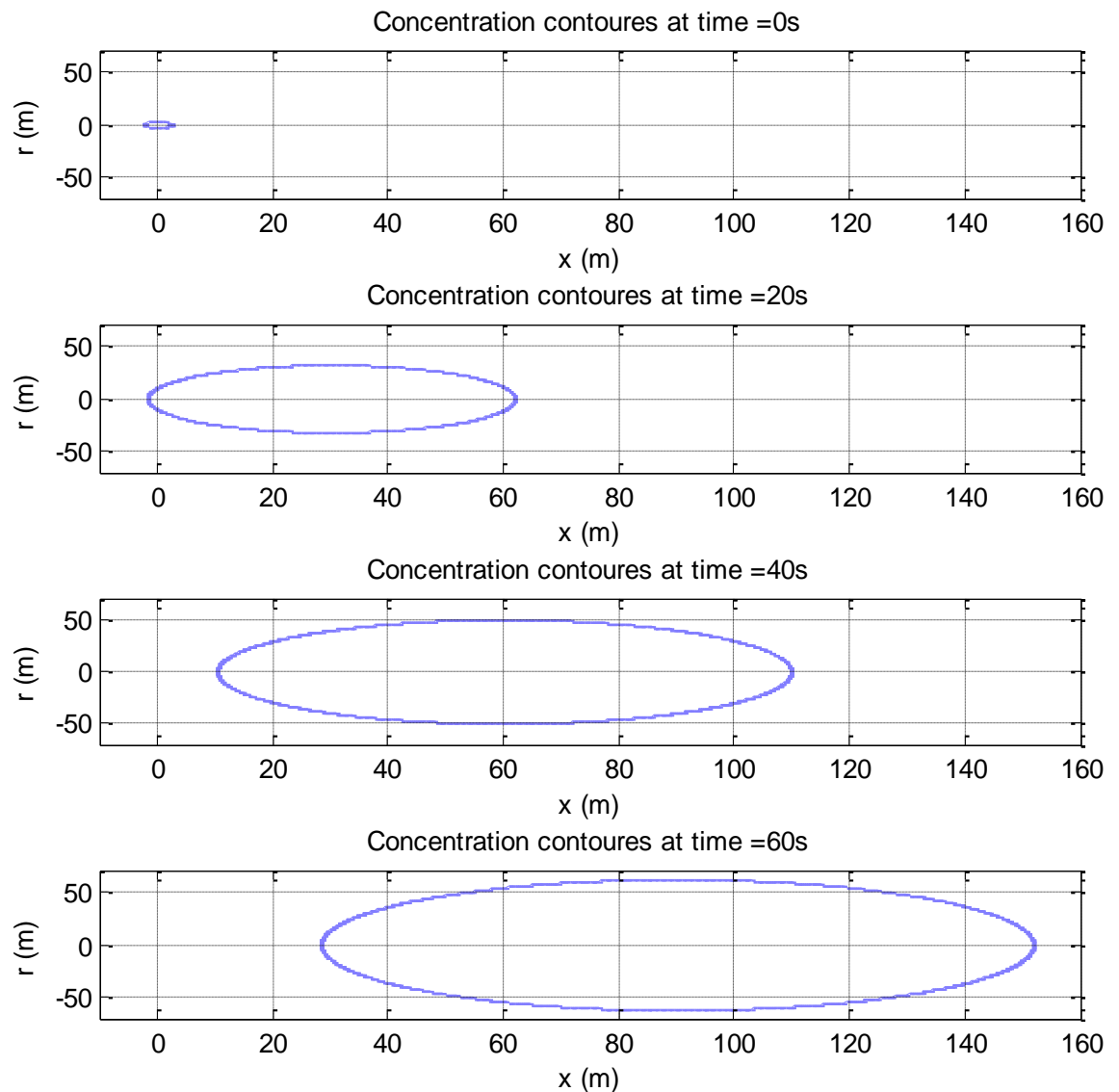


Figure 4.11 Propagation of contours in downwind direction

4.4 Safe Downwind Distance and Critical Time Interval

Safe Downwind Distance is the distance such that the concentration of the toxic material is minimized to the allowable value. As illustrated in figure 4.10, we can identify the safe downwind distance where the peak concentration is below the IDLH value.

Similarly critical time interval is the time period when the peak concentration is above the IDLH value. Therefore, using the concentration profiles, safe downwind distances and critical time intervals for different chlorine releases were calculated, and the results are shown in Table 4.1, and Figure 4.12.

Table 4.1 Safe downwind distances and Critical time intervals based on IDLH value

Amount released (Tons)	0.9	2	20	25	50	75	100
Safe Distance (km)	0.49	0.62	1.18	1.27	1.50	1.74	1.82
Time interval (min)	5.44	6.88	13.16	13.97	16.90	18.98	20.22

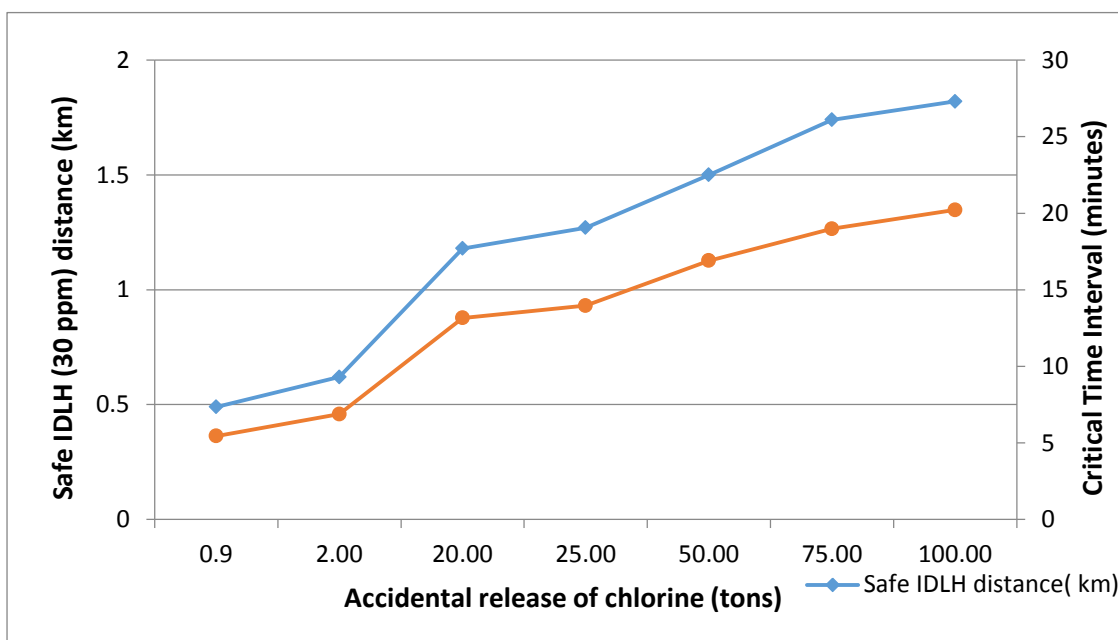


Figure 4.12 Safe IDLH distance and critical time period for different chlorine releases

According to the above Figure 4.12 we can see that for a 900kg release safe IDLH distance is above 490m and within that hazardous zone the critical time period is up to 5.44 minutes.

4.5 Probit Analysis of Model Results

In order to identify the effect of toxic release on humans, the relationship between the concentration profile and the degree of injury was established.

Probit equation given by Eisenberg, Lynch and Breeding for lethality is considered in the analysis, which is given by the following relation [11]:

$$Y = -17.1 + 1.69\ln(\Sigma C^{2.75}t) \quad (4.1)$$

Where:

Y = probit, (value range 2.67 – 8.09 representing 1 – 99.9% fatality) a measure of the percentage of the vulnerable resource that might sustain damage.

C = hazard concentration (ppm)

t = time in minutes

This relationship is applicable to healthy adults and susceptible individuals such as infants, elderly people and people with advanced pulmonary/cardiovascular disease.

From the probit graphs given in Chapter 2, Figure 2.5, for 30ppm (IDLH) concentration, no death is involved during the time interval 5.44 minutes, within the hazardous zone 490m. But according to Figure 2.6, 99.3% of the population is affected for chlorine injury for 30 ppm.

5 CONCLUSIONS

In this research a model was developed and applied to simulate an instantaneous chlorine gas release considering a location in Kalutara district. The work illustrates how heavy gas dispersion modeling techniques can be used for hazard analysis in cases where combined effect of gravity dominance and air entrainment is considered in an instantaneous release. In the present work, a worst case scenario study with Pasquill stability class A, has been conducted for an accidental release of 900kg of chlorine.

The model presented in this work can be used to model and simulate gas dispersion in the atmospheric environment for an instantaneous release of a heavy gas. Further this model can be used to predict information, concentration variation of the substance released with time, cloud dimensions such as height and radius and safe downwind distance.

The modeled results can be then used in determining the impact on people living in the vicinity of the released area. At different times after release, the ground level concentrations can be predicted and compared with tolerable concentrations of the substance concerned. The ground level distances from the point of release where the concentrations exceed the safe concentrations can be determined with this model. Further the length of time these harmful concentrations prevail can also be determined. Therefore, the impact on environment can be determined.

Application of this model to a chlorine gas release at a location in Kalutara district in Sri Lanka shows that after 5.44 minutes from the release of the gas, concentrations in the ground level have no impact on people. At this moment the downwind distance is 490m. This indicates that if there are no settlements within this distance from the industry releasing the chlorine gas people will not be affected harmfully.

5.1 Recommendations for future work

Using the modeled equations and data, simulation can be done for various parameters for impact assessment due to a heavy gas release. These results could be used for impact assessment studies during new plant developments. Further, the safe distances and critical time intervals determined from modeling could be used to warn people around the area to evacuate on time during an accident. The development of methodologies to incorporate these gas dispersion modeling to facilitate in above activities in Sri Lanka is a work that can be explored in the future.

Further development of user friendly tools on heavy gas dispersion that can facilitate Sri Lankan industry in complying to various regulations related to providing with adequate safety measures, proper storage facilities, and emergency planning is another area that needs further research.

REFERENCES

- [1] 2016. [Online]. Available: <http://www.adb.org/sites/default/files/project-document/71801/sri-kelanitissa.pdf>. [Accessed: 08- May- 2016].
- [2]P. Bourdeau and G. Green, Methods for assessing and reducing injury from chemical accidents. Chichester [England]: Wiley, 1989.
- [3]A. Chapman, Plume dispersion modeling of chlorine gas released due to ballistic attack on chlorine-carrying railway tanker. 2012.
- [4] "ELEVEN INJURED IN CHLORINE TANK EXPLOSION", The Daily Mirror (Colombo, Sri Lanka), 2012.
- [5]T. Bærland, "Release and Spreading of Dense Gases: Turbulence modeling with Kameleon FireEx", 2011.
- [6]"Gas Dispersion", <http://www.draeger.com/>. [Online]. Available: http://www.draeger.com/sites/assets/PublishingImages/Segments/ES/Oil-Gas-Industry/Plant-Safety-Operations/gas_dispersion_br_9046434_en.pdf. [Accessed: 08- May- 2016].
- [7]D. Crowl and J. Louvar, Chemical process safety. Englewood Cliffs, N.J.: Prentice Hall, 1990.
- [8]"INTRODUCTION TO ATMOSPHERIC DISPERSION MODELING". [Online]. Available: <http://www.envirometrics.com/abstracts/dismodel.pdf>. [Accessed: 08- May- 2016].
- [9]Approved Methods for the Modelling and Assessment of Air Pollutants in New South Wales, 1st ed. NSW: Department of Environment and Conservation, 2005.
- [10]"Methods of approximation and determination of human vulnerability for offshore major accident hazard assessment". [Online]. Available: http://www.hse.gov.uk/foi/internalops/hid_circs/technical_osd/spc_tech_osd_30/spctecosd30.pdf. [Accessed: 08- May- 2016].
- [11]F. Lees, Loss prevention in the process industries. London: Butterworths, 1980.

- [12]"Időjárás", Risk and hazard assessment for accidental chlorine release using dispersion modelling, vol. 102, no. 3, pp. 167-187, 1998.
- [13]E. Holzbecher, Environmental modeling. Berlin [u.a.]: Springer, 2007.
- [14]"The Gazette of the Democratic Socialist Republic of Sri Lanka", No. 1698/19 – Thursday March 24, 2011.
- [15] Ministry of State Resources and Enterprise Development, "Annual Report", Paranthan Chemicals Company Limited, 2013.
- [16][Online]. Available: <https://weather-and-climate.com/average-monthly-Rainfall-Temperature-Sunshine,kalutara,Sri-Lanka>. [Accessed: 08- May- 2016].
- [17]"Outline of air pollution dispersion", Wikipedia, 2016. [Online]. Available: https://en.wikipedia.org/wiki/Outline_of_air_pollution_dispersiion. [Accessed: 08-May- 2016].
- [18]P. Xuhai and J. Juncheng, Numerical Simulation Results on Instantaneous Release Dispersion of Heavy Gases, 1st ed. China.
- [19]M. Mohan, T. Panwar and M. Singh, Development of dense gas dispersion model for emergency preparedness, 1st ed. 1995.
- [20]J. McQuaid and B. Roebuck, Large scale field trials on dense vapour dispersion. Luxembourg: Office for Official Publications of the European Communities, 1985.
- [21]Guidelines for chemical process quantitative risk analysis. New York: The Center, 2000.
- [22]"List of atmospheric dispersion models", Wikipedia, 2016. [Online]. Available: https://en.wikipedia.org/wiki/List_of_atmospheric_dispersiion_models. [Accessed: 17- Jul- 2016].
- [23]S. Coldrick, C. Lea and M. Ivings, Validation database for evaluating vapor dispersion models for safety analysis of LNG facilities. Quincy, MA: Fire Protection Research Foundation, 2009.

APPENDICES

APPENDIX A – Supporting calculation excel for the Matlab m files

	A	B	C	D	E	F	G	H	I	J	K	L	M
1	Supporting calculation for the Matlab m files												
2													
3	Air velocity	u	=	1.5	m/s								
4	Initial toxic mass	Mg	=	900	kg								
5	Constant	C	=	1.3									
6	Gas density	Pg	=	3.214	kg/m3								
7	Air density	Pa	=	1.225	kg/m3								
8	Gravitational constant	g	=	9.81	m/s2								
9													
10													
11	$dr/dt = C*(gh(Pg-Pa)/Pa)^{0.5}$												
12													
13		A	=	3.203113378									
14													
15	dr/dt	=	Asqrt(h)										
16													
17	Gravity slumping phase:												
18	Assumption:												
19	At t=0 radius and height is equal.												
20													
21	$V_0 = Mg/Pg$												
22		V_0	=	280.0248911	m3								
23													
24	$V = \pi*r^2*h$												
25													
26													
27													
28													
29													
30													
31													
32													
33													
34													
35		U^*/u	=	0.1									
36		U^*	=	0.15									
37													
38	Entrainment velocity	U_e											
39													
40	$U_e = \alpha * U_1 / Ri$												
41													
42		α	=	0.6									
43		α^2	=	0.5									
44	Turbulence velocity	U_1											
45													
46													
47													
48													
49													
50													
51	Richardson number												
52													
53	$Ri = (gls/U_1^2)*(Pg-Pa)/Pg$												
54		Ri_0	=	1271.218613									
55													
56													
57													
58	$dMa/dt = Pa(\pi*r^2)U_e + 2Pa(\pi*r^2)*\alpha^2*(dr/dt)$												
59	$dMa/dt = Pa(\pi*r^2)(\alpha*U_1/Ri) + 2Pa(\pi*r^2)*\alpha^2*(dr/dt)$												
60	$dMa/dt = Pa(\pi*r^2)(\alpha*U_1^3*Pg/(g*5.88*h^{0.48}*detlaP) + 2Pa(\pi*r^2)*\alpha^2*(dr/dt)$												
61													
62		dMa/dt	=	0.000894202	$r^2/h^{0.48} +$	3.848451	r^2*dr/dt						
63		dMa/dt	=	0.000894202	$r^2/h^{0.48} +$	12.32702	$r^2*h^{1.5}$						
64													
65	$dMa/dt = Pa(\pi*r^2)dh/dt + 2Pa(\pi*r^2)*(dr/dt)$												
66													
67		dMa/dt	=	3.848451001	$*r^2*dh/dt +$	7.696902	$*r^2*dr/dt$						
68													
69													
70													
71		3.848451001	$*r^2*dh/dt +$	7.696902	$*r^2*dr/dt$	=	0.000894	$r^2/h^{0.48} +$	3.848451	r^2*dr/dt			
72													
73		3.848451	$*r^2*dh/dt$			=	0.000894	$r^2/h^{0.48} +$	3.848451	r^2*dr/dt	-	7.696902	$*r^2*dr/dt$
74		3.848451	$*r^2*dh/dt$			=	0.000894	$r^2/h^{0.48} +$	-3.848451	r^2*dr/dt			
75													
76					dh/dt	=	0.000232	$/h^{0.48}$	-3.20311	$h^{1.5}/r$			
77													
78		B =		0.000232									
79		D =		-3.20311									
80		E =		0.000894									
81		F =		12.32702									
82													

APPENDIX B – mfile for entrainment phase

```
%Air entrainment phase R , H and Ma vs time graphs

%define variables for Equation 1 ( $r'=A*h^{0.5}$ )
clear all;
% read excel for variables
filename = 'calculation.xlsx';
sheet = 1;
xlRange = 'D3:D8';
subsetA1 = xlsread(filename,sheet,xlRange);

u = subsetA1(1);
Mg = subsetA1(2);
C = 1.3;
Pg = 3.214;
Pa = 1.225;
g = 9.81;

A = C*(g*(Pg-Pa)/Pg)^0.5;

xlRange = 'C78:C81';
subsetA2 = xlsread(filename,sheet,xlRange);

%define variables for Equation 2 ( $h'=B/h^{0.48}+D*h^{1.5}/r$ )

B=subsetA2(1);
D=subsetA2(2);

%define variables for Equation 3 ( $dMa/dt=E*r^2/h^{0.48}+F*r*h^{1.5}$ )

E=subsetA2(3);
F=subsetA2(4);

xlRange = 'D29';
subsetA3 = xlsread(filename,sheet,xlRange);
```

```

r0 = subsetA3(1);
h0 = subsetA3(1);

%ODE solver
t1=0:0.1:900;
funch = @(T,x) [A*x(2)^0.5; B*x(2)^(-0.48)+D*(x(2)^1.5)/x(1);
E*x(1)^2/x(2)^0.48+F*x(1)*x(2)^1.5];
[t1,RHM_VAL] = ode45(funch, t1, [r0 h0 0]);

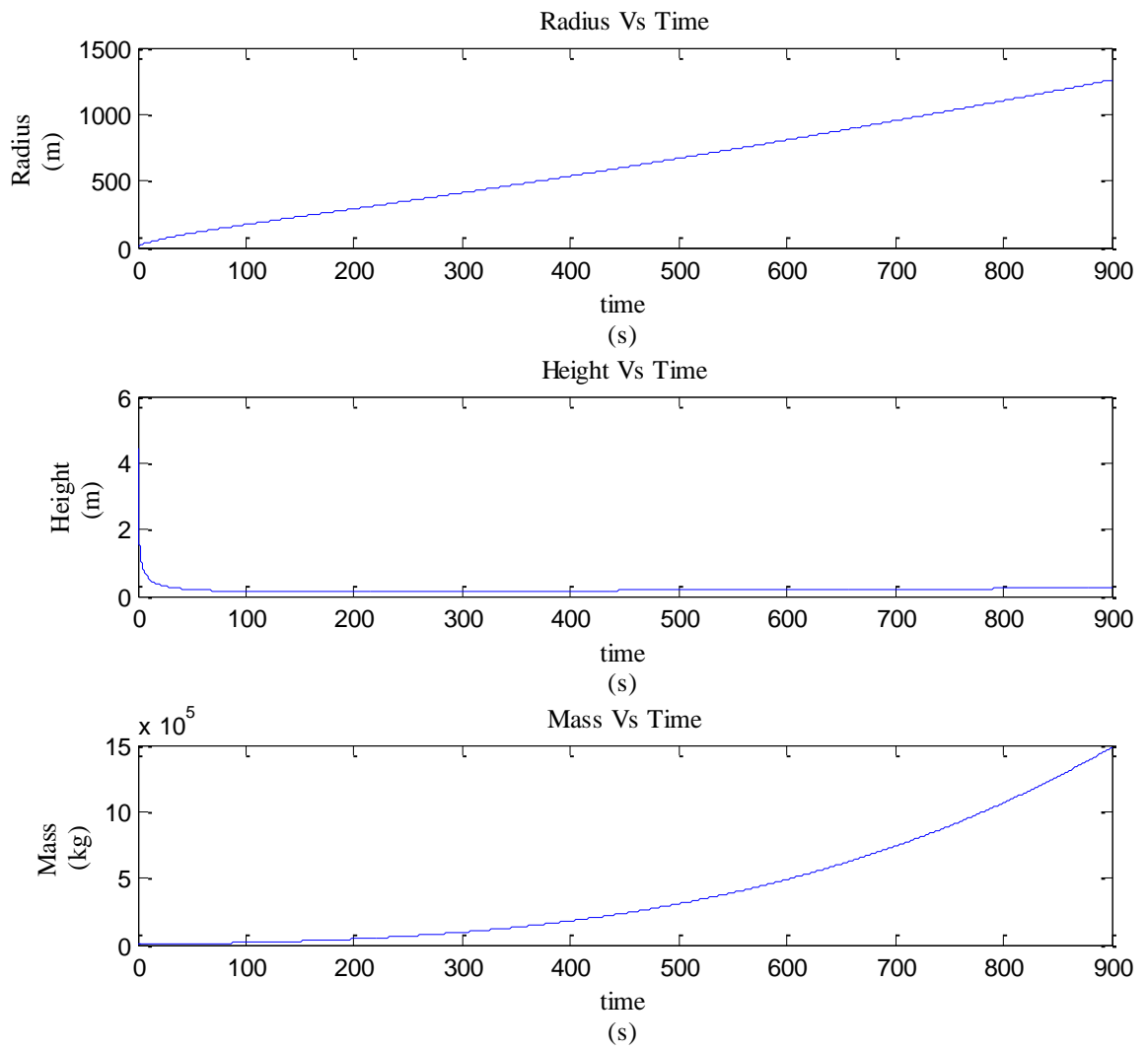
r1 = RHM_VAL(:,1);
h1 = RHM_VAL(:,2);
m1 = RHM_VAL(:,3);

%plot time vs radius
subplot(3,1,1)
plot(t1,RHM_VAL(:,1), 'b-');
xlabel({'time', '(s)'});
ylabel({'Radius', '(m)'});
title('Radius Vs Time');

%plot time vs height
subplot(3,1,2)
plot(t1,RHM_VAL(:,2), 'b-');
title('Height Vs Time');
xlabel({'time', '(s)'});
ylabel({'Height', '(m)'});

%plot time vs mass
subplot(3,1,3)
plot(t1,RHM_VAL(:,3), 'b-');
title('Mass Vs Time');
xlabel({'time', '(s)'});
ylabel({'Mass', '(kg)'});

```



Graphs of (a) Radius vs Time (b) Height vs Time (c) Mass vs Time in entrainment phase

APPENDIX C- mfile for post transition period

```
%Post transition phase R and H vs time graphs

%define variables for Equation 1 ( $r'=A*h^{0.5}$ )
clear all;
% read excel for variables
filename = 'calculation.xlsx';
sheet = 1;
xlRange = 'D3:D8';
subsetA1 = xlsread(filename,sheet,xlRange);

u = subsetA1(1);
Mg = subsetA1(2);
C = 1.3;
Pg = 3.214;
Pa = 1.225;
g = 9.81;
U_fr = 0.1 * u;
alpha2 = 0.5;

A = C*(g*(Pg-Pa)/Pg)^0.5;

xlRange = 'C78:C81';
subsetA2 = xlsread(filename,sheet,xlRange);

%define variables for Equation 2 ( $h'=B/h^{0.48}+D*h^{1.5}/r$ )

B=subsetA2(1);
D=subsetA2(2);

%define variables for Equation 3 ( $dMa/dt=E*r^2/h^{0.48}+F*r*h^{1.5}$ )

E=subsetA2(3);
```

```

F=subsetA2(4);

xlRange = 'D29';
subsetA3 = xlsread(filename,sheet,xlRange);

r0 = subsetA3(1);
h0 = subsetA3(1);

%ODE solver
t1=0:1:1200;
funch = @(T,x) [A*x(2)^0.5; B*x(2)^(-0.48)+D*(x(2)^1.5)/x(1);
E*x(1)^2/x(2)^0.48+F*x(1)*x(2)^1.5];
[t1,RHM_VAL] = ode45(funch, t1, [r0 h0 0]);

r1 = RHM_VAL(:,1);
h1 = RHM_VAL(:,2);
m1 = RHM_VAL(:,3);

M = Mg+m1;
V = Mg/Pg+m1/Pa;

rho = M./V;
[ row,col] = size(rho);

idx = 1;
while idx < row && ((rho(idx)-Pa)>0.001 )
% print(i);
idx = idx + 1;
end

t_T = t1(idx);
r_T = r1(idx);
h_T = h1(idx);

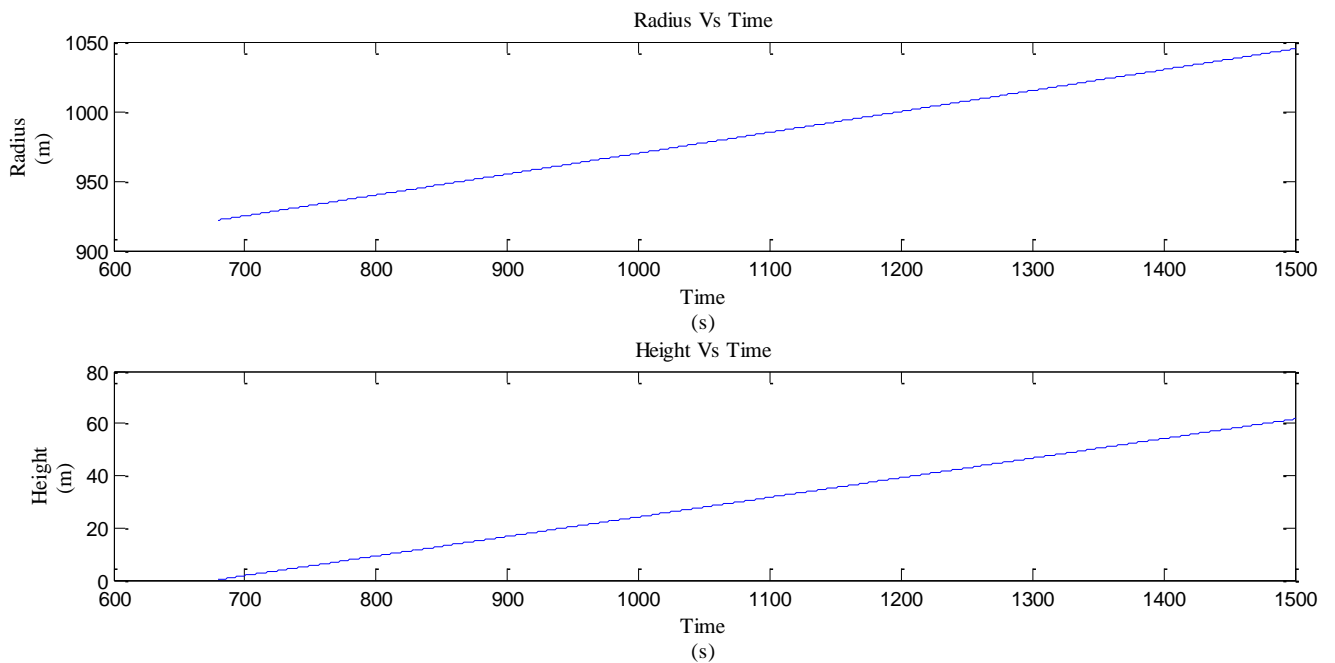
t2 = t_T : 1 : 1500;

```

```
r2 = r_T + U_fr * (t2 - t_T);  
h2 = h_T + alpha2 * U_fr * (t2 - t_T);
```

```
% plot time vs radius  
subplot(2,1,1)  
plot(t2, r2, 'b-');  
xlabel({'time', '(s)'});  
ylabel({'Radius', '(m)'});  
title('Radius Vs Time');
```

```
%plot time vs height  
subplot(2,1,2)  
plot(t2, h2, 'b-');  
title('Height Vs Time');  
xlabel({'time', '(s)'});  
ylabel({'Height', '(m)'});
```



Graphs of (a) Radius vs Time (b) Height vs Time in post transition phase

APPENDIX D - mfile for all three phases

```
%define variables for Equation 1 ( $r'=A*h^{0.5}$ )
clear all;
% read excel for variables
filename = 'calculation.xlsx';
sheet = 1;
xlRange = 'D3:D8';
subsetA1 = xlsread(filename,sheet,xlRange);

u = subsetA1(1);
Mg = subsetA1(2);
C = 1.3;
Pg = 3.214;
Pa = 1.225;
g = 9.81;
U_fr = 0.1 * u;
alpha2 = 0.5;

A = C*(g*(Pg-Pa)/Pg)^0.5;

xlRange = 'C78:C81';
subsetA2 = xlsread(filename,sheet,xlRange);

%define variables for Equation 2 ( $h'=B/h^{0.48}+D*h^{1.5}/r$ )

B=subsetA2(1);
D=subsetA2(2);

%define variables for Equation 3 ( $dMa/dt=E*r^2/h^{0.48}+F*r*h^{1.5}$ )

E=subsetA2(3);
F=subsetA2(4);

xlRange = 'D29';
subsetA3 = xlsread(filename,sheet,xlRange);
```

```

r0 = subsetA3(1);
h0 = subsetA3(1);

%ODE solver
t1=0:1:1200;

funch = @(T,x) [A*x(2)^0.5; B*x(2)^(-0.48)+D*(x(2)^1.5)/x(1);
E*x(1)^2/x(2)^0.48+F*x(1)*x(2)^1.5];

[t1,RHM_VAL] = ode45(funch, t1, [r0 h0 0]);

r1 = RHM_VAL(:,1);
h1 = RHM_VAL(:,2);
m1 = RHM_VAL(:,3);

M = Mg+m1;
V = Mg/Pg+m1/Pa;

rho = M./V;

[row,col] = size(rho);

idx = 1;
while idx < row && ((rho(idx)-Pa)>0.001 )
% print(i);
    idx = idx + 1;
end

t_T = t1(idx);
r_T = r1(idx);
h_T = h1(idx);

t2 = t_T : 1 : 1200;
r2 = r_T + U_fr * (t2 - t_T);
h2 = h_T + alpha2 * U_fr * (t2 - t_T);

%t_m = [t1';t2(1:idx)]; % combining phase1 and phase2
t_final = [t1(1:idx); t2'];
r_final = [r1(1:idx);r2'];

```

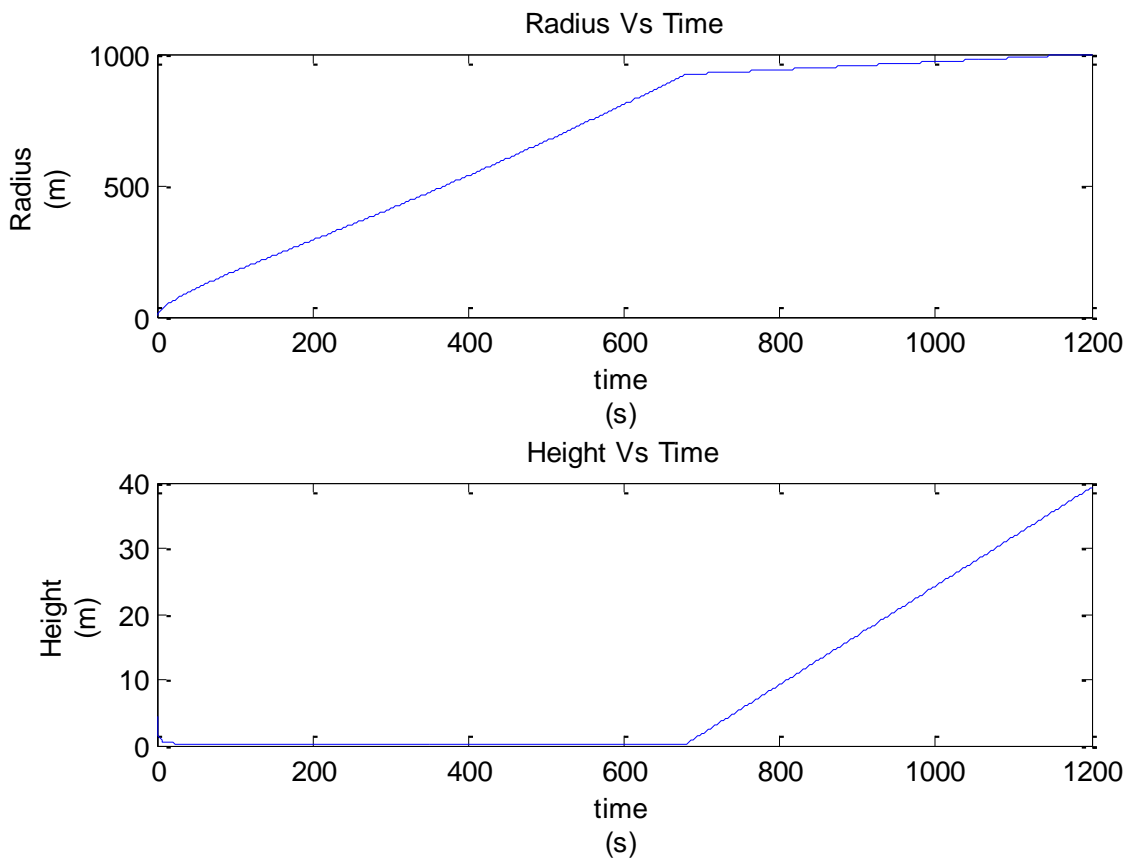
```

h_final = [h1(1:idx);h2'];
m_final = m1(1:idx);

%plot time vs radius
subplot(2,1,1)
plot(t_final, r_final, 'b-');
title('Radius Vs Time');
xlabel({'time', '(s)'});
ylabel({'Radius', '(m)'});

%plot time vs height
subplot(2,1,2)
plot(t_final, h_final, 'b-');
title('Height Vs Time');
xlabel({'time', '(s)'});
ylabel({'Height', '(m)'});

```



Graphs of (a) Radius vs Time (b) Height vs Time in all three phases

APPENDIX E – mfile for concentration profile

```
%define variables for Equation 1 ( $r'=A*h^{0.5}$ )
clear all;

% read excel for variables
filename = 'calculation.xlsx';
sheet = 1;
xlRange = 'D3:D8';
subsetA1 = xlsread(filename,sheet,xlRange);

u = subsetA1(1);
Mg = subsetA1(2);
C = 1.3;
Pg = 3.214;
Pa = 1.225;
g = 9.81;
U_fr = 0.1 * u;
alpha2 = 0.5;

A = C*(g*(Pg-Pa)/Pg)^0.5;

xlRange = 'C78:C81';
subsetA2 = xlsread(filename,sheet,xlRange);

%define variables for Equation 2 ( $h'=B/h^{0.48}+D*h^{1.5}/r$ )

B=subsetA2(1);
D=subsetA2(2);

%define variables for Equation 3 ( $dMa/dt=E*r^2/h^{0.48}+F*r*h^{1.5}$ )

E=subsetA2(3);
F=subsetA2(4);
```

```

xlRange = 'D29';
subsetA3 = xlsread(filename, sheet, xlRange);

r0 = subsetA3(1);
h0 = subsetA3(1);

%ODE solver
t1=0:0.1:1000;
funch = @(T,x) [A*x(2)^0.5; B*x(2)^(-0.48)+D*(x(2)^1.5)/x(1);
E*x(1)^2/x(2)^0.48+F*x(1)*x(2)^1.5];
[t1,RHM_VAL] = ode45(funch, t1, [r0 h0 0]);

r1 = RHM_VAL(:,1);
h1 = RHM_VAL(:,2);
m1 = RHM_VAL(:,3);

M = Mg+m1;
V = Mg/Pg+m1/Pa;

rho = M./V;
[row,col] = size(rho);

idx = 1;
while idx < row && ((rho(idx)-Pa)>0.001 )
% print(i);
    idx = idx + 1;
end

t_T = t1(idx);
r_T = r1(idx);
h_T = h1(idx);

t2 = t_T : 1 : 1500;
r2 = r_T + U_fr * (t2 - t_T);
h2 = h_T + alpha2 * U_fr * (t2 - t_T);

```

```

t_final = [t1(1:idx); t2'];
r_final = [r1(1:idx);r2'];
h_final = [h1(1:idx);h2'];
m_final = m1(1:idx);

sigmay = r_final / 2.14;
sigmaz = h_final / 2.14;

colors = {'-b' '-g' '-r' '-c' '-m'};
legendInfo = {};
plots = {};
for n = 1:3

    t_index = (n)*1000;
    t = t_final(t_index);

[x,y,z] = meshgrid(-150:5:1000,-50:5:500,0:0.1:3);
G = exp (-(((y.^2) + ((x-(u*t)).^2))/(2*(sigmay(t_index)^2))) -
((z.^2)/(2*(sigmaz(t_index)^2))));
C = Mg*G/(sqrt(2)*(pi^1.5)*(sigmay(t_index)^2)*sigmaz(t_index));
Z = C(:,:,1);
[rw,col] = size(Z);

%X = ones(rw,col);
[Xa,Y] = meshgrid(-150:5:1000,-50:5:500);
Y = Z(1,:);
X = Xa(1,:);
plot(X,Y , colors{n});
indexmax = find(max(Y) == Y);
xmax = X(indexmax);
ymax = Y(indexmax);

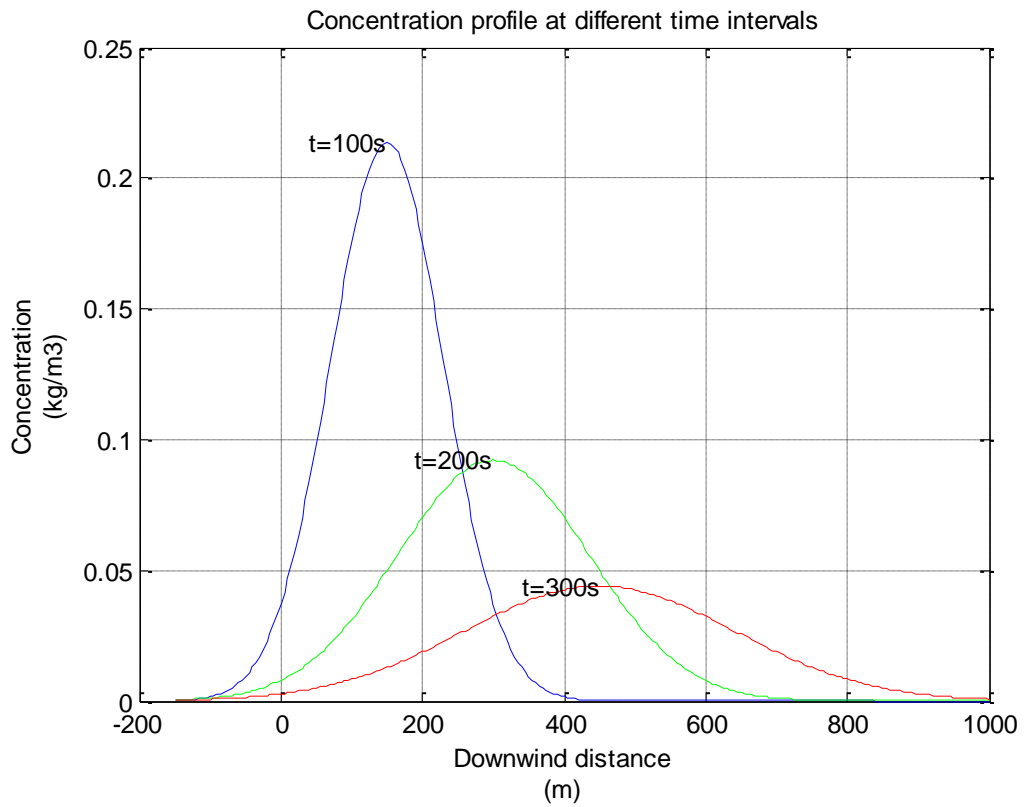
strmax = strcat('t=' , num2str(round(t)), 's');
text(xmax,ymax,strmax, 'HorizontalAlignment', 'right');

```

```
title('Concentration profile at different time intervals');
xlabel({'Downwind distance','(m)'});
ylabel({'Concentration','(kg/m3)'});

hold on;
end

grid on
```



Concentration profile at different times after the release

APPENDIX F - m file for contour curves

```
%define variables for Equation 1 (r'=A*h^0.5)
clear all;
% read excel for variables
filename = 'calculation.xlsx';
sheet = 1;
xlRange = 'D3:D8';
subsetA1 = xlsread(filename,sheet,xlRange);

u = subsetA1(1);
Mg = subsetA1(2);
C = 1.3;
Pg = 3.214;
Pa = 1.225;
g = 9.81;
U_fr = 0.1 * u;
alpha2 = 0.5;

A = C*(g*(Pg-Pa)/Pg)^0.5;

xlRange = 'C78:C81';
subsetA2 = xlsread(filename,sheet,xlRange);

%define variables for Equation 2 (h'=B/h^0.48+D*h^1.5/r)

B=subsetA2(1);
D=subsetA2(2);

%define variables for Equation 3 (dMa/dt=E*r^2/h^0.48+F*r*h^1.5)

E=subsetA2(3);
F=subsetA2(4);

xlRange = 'D29';
subsetA3 = xlsread(filename,sheet,xlRange);

r0 = subsetA3(1);
h0 = subsetA3(1);

%ODE solver
t1=0:0.1:1000;
funch = @(T,x) [A*x(2)^0.5; B*x(2)^(-0.48)+D*(x(2)^1.5)/x(1);
E*x(1)^2/x(2)^0.48+F*x(1)*x(2)^1.5];
[t1,RHM_VAL] = ode45(funch, t1, [r0 h0 0]);

r1 = RHM_VAL(:,1);
h1 = RHM_VAL(:,2);
m1 = RHM_VAL(:,3);
%===== end of
phase1=====
```



```

M = Mg+m1;
V = Mg/Pg+m1/Pa;

rho = M./V;

[row,col] = size(rho);

%for idx = 1:1:row
%   if(rho(idx)<1.2251 && rho(idx)>1.2250)
%       % t_post = t(idx);
%       %disp( t(idx));
%       break
%   end
%end
idx = 1;
while idx < row && ((rho(idx)-Pa)>0.001 )
%   print(i);
    idx = idx + 1;
end

t_T = t1(idx);
r_T = r1(idx);
h_T = h1(idx);

t2 = t_T : 1 : 1500;
r2 = r_T + U_fr * (t2 - t_T);
h2 = h_T + alpha2 * U_fr * (t2 - t_T);

t_final = [t1(1:idx); t2'];
r_final = [r1(1:idx); r2'];
h_final = [h1(1:idx); h2'];
m_final = m1(1:idx);

sigmay = r_final / 2.14;
sigmaz = h_final / 2.14;

for n = 1:2:8
    %n = 2;
    %t_index = (n-1)*2+1;
    t_index = (n-1)*100+1;
    t = t_final(t_index);
    disp(t);
    [x,y,z] = meshgrid(-10:0.5:160,-70:0.5:70,0:0.1:3);
    G = exp (-(((y.^2) + ((x-(u*t)).^2))/(2*(sigmay(t_index)^2))) -
    ((z.^2)/(2*(sigmaz(t_index)^2))));
    C = Mg*G/(sqrt(2)*(pi^1.5)*(sigmay(t_index)^2)*sigmaz(t_index));
    Z = C(:, :, 1);
    [rw,col] = size(Z);
    colormap cool;

```

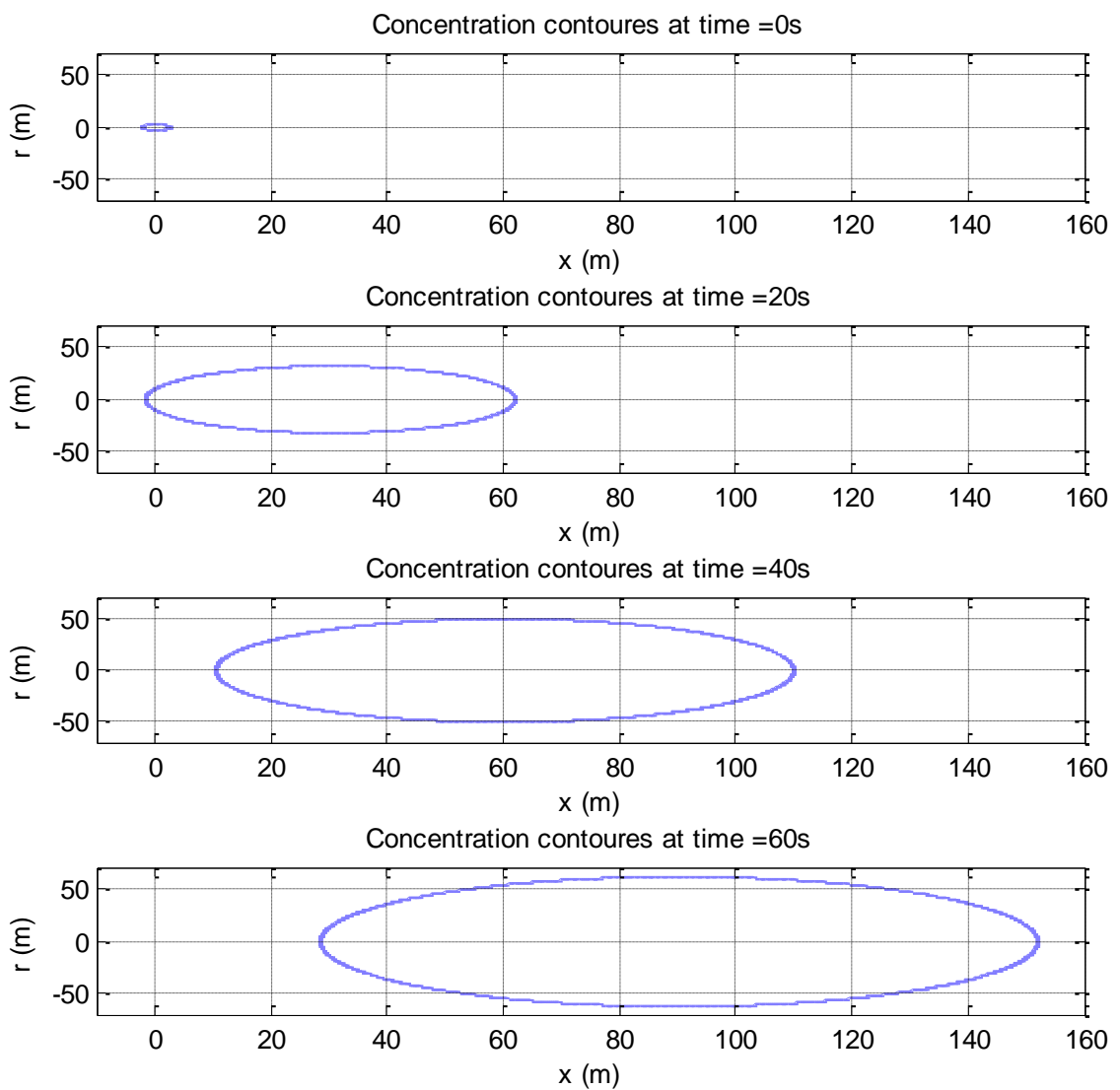
```

inx = (n+1)/2;
subplot(4,1,inx);
[X,Y] = meshgrid(-10:.5:160,-70:.5:70);
[c,h] = contour(X,Y,Z,1);
str = strcat('Concentration contours at time = ', num2str(t),
's');

title(str);
xlabel({'x (m)'});
ylabel({'r (m)'});
hold on;
grid on;

end

```



Propagation of contours in downwind direction

APPENDIX G- Probit calculation Excel sheet

Percentage Fatalities from a Fixed Concentration-Time Relationship Example:

Input Data:

Concentration: 30 Ppm
 Exposure Time: 260 minutes
 Probit Equation:
 k1: -17.1
 k2: 1.69
 Exponent: 2.75

Equation for Fatality:

$$Y = -17.1 + 1.69\ln(\Sigma C^{2.75}t)$$

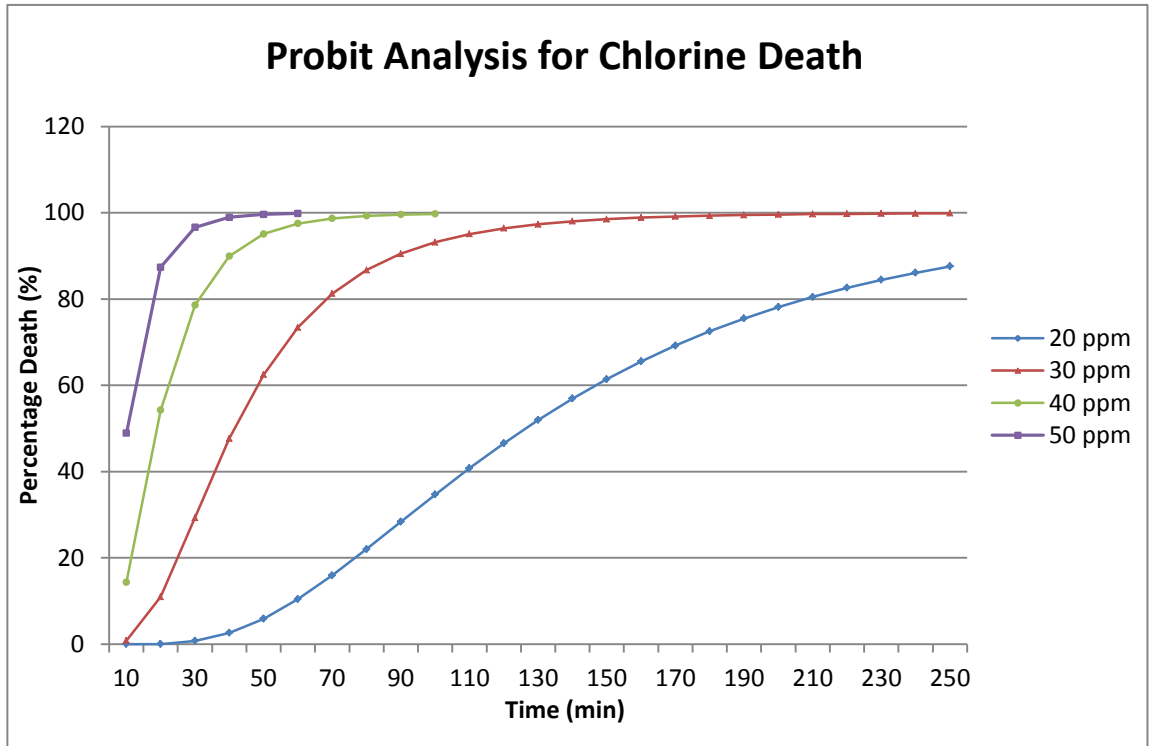
Calculated Results:

Probit Value (Y): 8.10
 Percent: 99.90 %

Concentration @ 20 ppm		Concentration @ 30 ppm		Concentration @ 40 ppm		Concentration @ 50 ppm	
Time (min)	Percentage of Death (%)	Time (min)	Percentage of Death (%)	Time (min)	Percentage of Death (%)	Time (min)	Percentage of Death (%)
10	0	10	0.82	10	14.35	10	48.9
20	0	20	10.93	20	54.25	20	87.37
30	0.76	30	29.29	30	78.58	30	96.63
40	2.6	40	47.66	40	89.94	40	98.97
50	5.87	50	62.49	50	95.11	50	99.65
60	10.42	60	73.45	60	97.52	60	99.87
70	15.93	70	81.25	70	98.69		
80	22.01	80	86.71	80	99.29		
90	28.34	90	90.52	90	99.6		
100	34.66	100	93.19	100	99.76		
110	40.77	110	95.06				

120	46.55
130	51.95
140	56.91
150	61.43
160	65.53
170	69.22
180	72.53
190	75.49
200	78.14
210	80.49
220	82.59
230	84.45
240	86.1
250	87.57

120	96.39
130	97.34
140	98.02
150	98.52
160	98.88
170	99.15
180	99.35
190	99.5
200	99.61
210	99.7
220	99.76
230	99.81
240	99.85
250	99.88
260	99.9

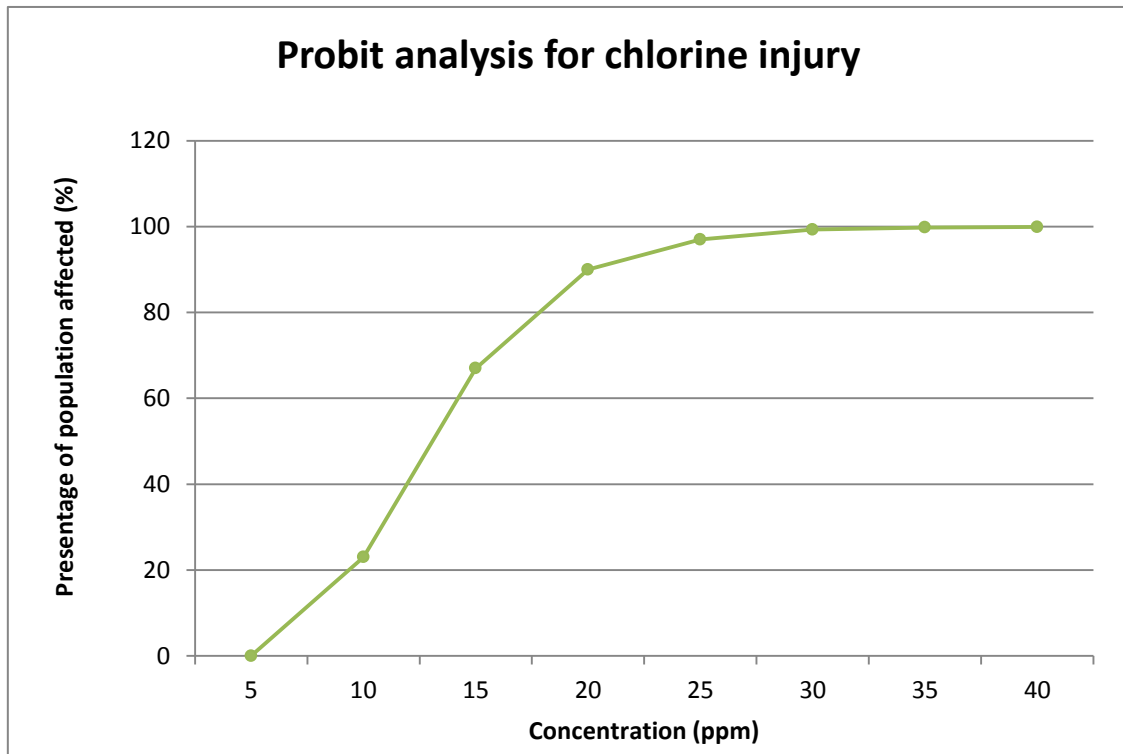


Probit analysis for chlorine injury

Probit equation for non-lethal injury:

$$Y = -2.40 + 2.90 \ln(C)$$

C	Y	%
5	2.26736995	0
10	4.27749677	23
15	5.45334558	67
20	6.28762359	90
25	6.93473989	97
30	7.46347241	99.3
35	7.91050938	99.8
40	8.29775042	99.9



Probit analysis for chlorine injury

APPENDIX H – Model validation and sensitivity analysis of parameters

Parameters C , α^* , α , U^*/U are varied to obtain the optimum validation results. Best values were obtained from test 8.

Table: Values varied in sensitivity analysis

	C	α^*	α	U^*/U
test1	1.00	0.50	0.20	0.10
test2	1.00	0.50	0.45	0.10
test3	1.00	0.50	0.50	0.10
test4	1.00	0.50	0.60	0.10
test5	1.30	0.50	0.50	0.10
test6	1.30	0.50	0.50	0.20
test7	1.30	0.50	0.60	0.10
test8	1.30	0.60	0.50	0.10
test9	1.30	0.70	0.50	0.10

The obtained results (error %) is shown in below table:

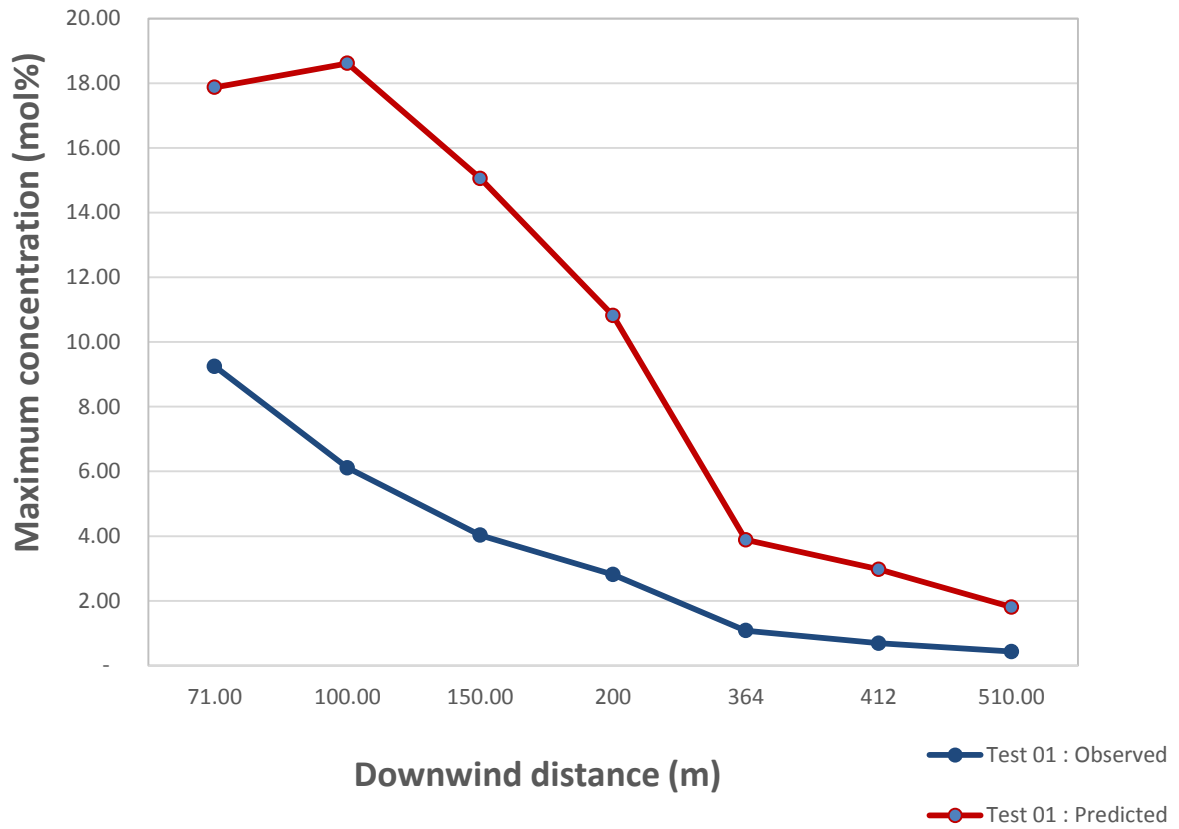
Test 1:

C = 1.00

 $\alpha^* = 0.50$ $\alpha = 0.20$ $U^*/U = 0.10$

X(m)	T(s)	t_ind ex	gas conc.	gas M (kg/ mol)	gas conc mol	r	h	ma	v	rho air	air M (kg/ mol)	air conc.	mol%	obse rved mol %	error %
71	29.9	300	0.71090	120	0.005924	65.19	0.4258	4,489	5,684.83	0.7896	29	0.0272	17.87	9.25	48.23
100	41.7	418	0.84270	120	0.007023	79.90	0.3765	6,725	7,551.07	0.8906	29	0.0307	18.61	6.11	67.17
150	61.9	620	0.74800	120	0.006233	103.50	0.3639	12,490	12,246.52	1.0199	29	0.0352	15.06	4.03	73.23
200	83.9	840	0.55190	120	0.004599	129.60	0.3819	22,160	20,151.60	1.0997	29	0.0379	10.82	2.81	74.02
364	151.9	1,520	0.19880	120	0.001657	216.00	0.4745	82,630	69,549.43	1.1881	29	0.0410	3.89	1.08	72.21
412	171.9	1,720	0.15180	120	0.001265	243.30	0.5027	111,900	93,485.22	1.1970	29	0.0413	2.97	0.69	76.80
510	212.9	2,130	0.09199	120	0.000767	302.90	0.5603	195,100	161,498.70	1.2081	29	0.0417	1.81	0.43	76.20

Observed and predicted maximum concentration at various downwind distances for Test 01



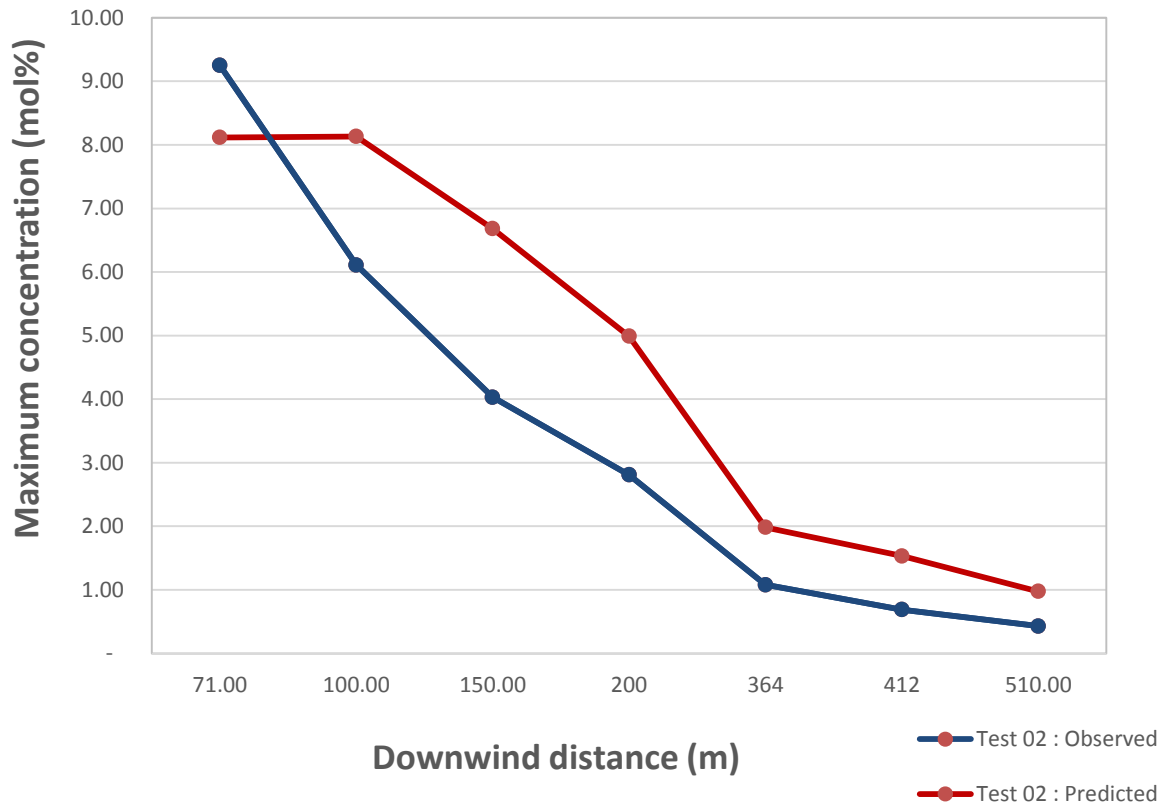
Test 2:

C = 1.00

 $\alpha^* = 0.50$ $\alpha = 0.45$ $U^*/U = 0.10$

X(m)	T(s)	t_ind ex	gas conc.	gas M (kg/ mol)	gas conc mol	r	h	ma	v	rho air	air M (kg/ mol)	air conc.	mol %	observ ed mol%	error %
71	29.9	300	0.39360	120	0.003280	80.94	0.80360	17,810	16,539.26	1.0768	29	0.03713	8.12	9.25	(13.97)
100	41.7	418	0.40710	120	0.003393	100.70	0.68480	24,250	21,815.87	1.1116	29	0.03833	8.13	6.11	24.86
150	61.9	620	0.34080	120	0.002840	132.00	0.60230	37,930	32,969.37	1.1505	29	0.03967	6.68	4.03	39.68
200	83.9	840	0.25520	120	0.002127	164.90	0.58040	58,220	49,581.38	1.1742	29	0.04049	4.99	2.81	43.69
364	151.9	1,520	0.10110	120	0.000843	267.40	0.63470	172,200	142,574.28	1.2078	29	0.04165	1.98	1.08	45.53
412	171.9	1,720	0.07800	120	0.000650	298.80	0.66130	224,700	185,485.34	1.2114	29	0.04177	1.53	0.69	54.97
510	212.9	2,130	0.04966	120	0.000414	365.10	0.71930	366,500	301,219.86	1.2167	29	0.04196	0.98	0.43	55.98

Observed and predicted maximum concentration at various downwind distances for Test 02



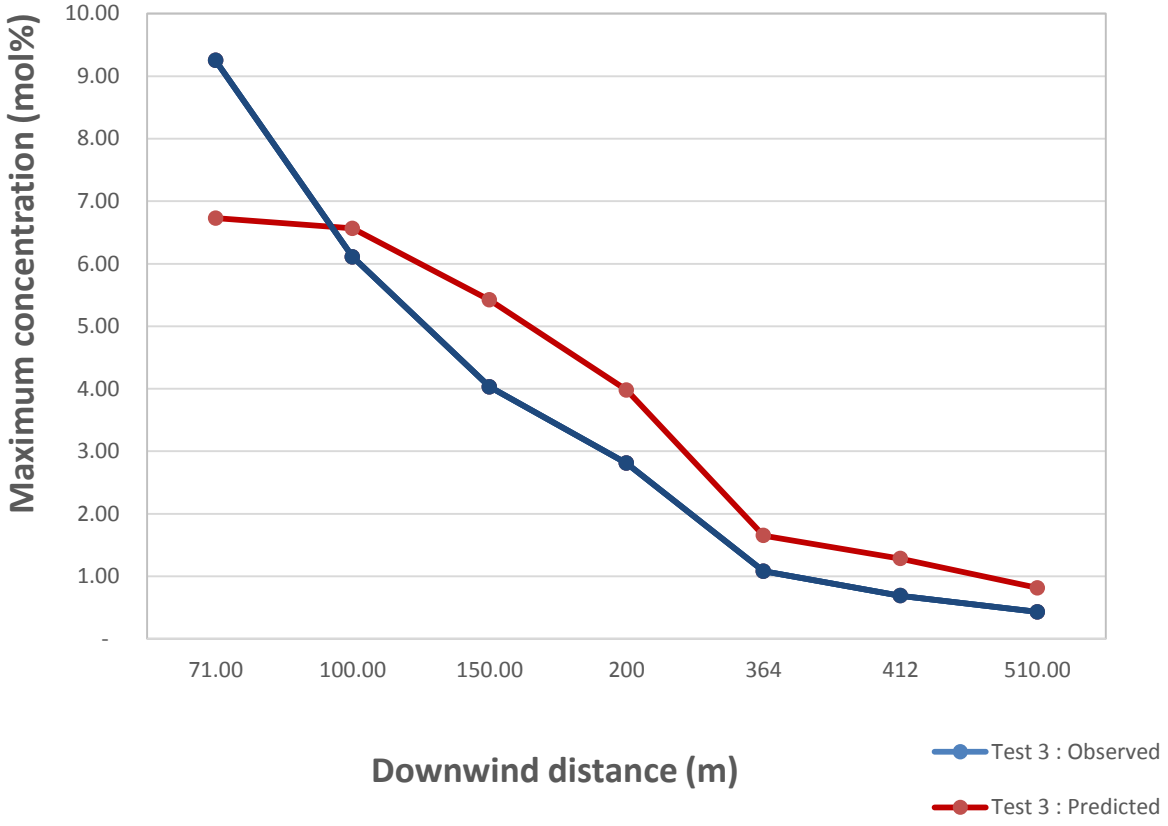
Test 3:

C = 1.00

 $\alpha^* = 0.50$ $\alpha = 0.50$ $U^*/U = 0.10$

X(m)	T(s)	t_ind ex	gas conc.	gas M (kg/ mol)	gas conc mol	r	h	ma	v	rho air	air M (kg/ mol)	air conc.	mol %	obser ved mol%	error %
71	29.9	300	0.33140	120	0.002762	85.24	0.93800	23,770	21,411.13	1.1102	29	0.03828	6.73	9.25	(37.47)
100	41.7	418	0.33070	120	0.002756	106.60	0.79950	32,470	28,541.89	1.1376	29	0.03923	6.56	6.11	6.92
150	61.9	620	0.27120	120	0.002260	140.40	0.69540	49,260	43,064.44	1.1439	29	0.03944	5.42	4.03	25.63
200	83.9	840	0.20340	120	0.001695	175.50	0.65890	75,620	63,756.38	1.1861	29	0.04090	3.98	2.81	29.39
364	151.9	1,520	0.08295	120	0.000691	283.60	0.69370	209,400	175,280.67	1.1947	29	0.04120	1.65	1.08	34.56
412	171.9	1,720	0.06532	120	0.000544	316.30	0.71800	274,000	225,669.41	1.2142	29	0.04187	1.28	0.69	46.24
510	212.9	2,130	0.04165	120	0.000347	385.20	0.77000	439,400	358,932.81	1.2242	29	0.04221	0.82	0.43	47.27

Observed and predicted maximum concentration at various downwind distances for Test 03



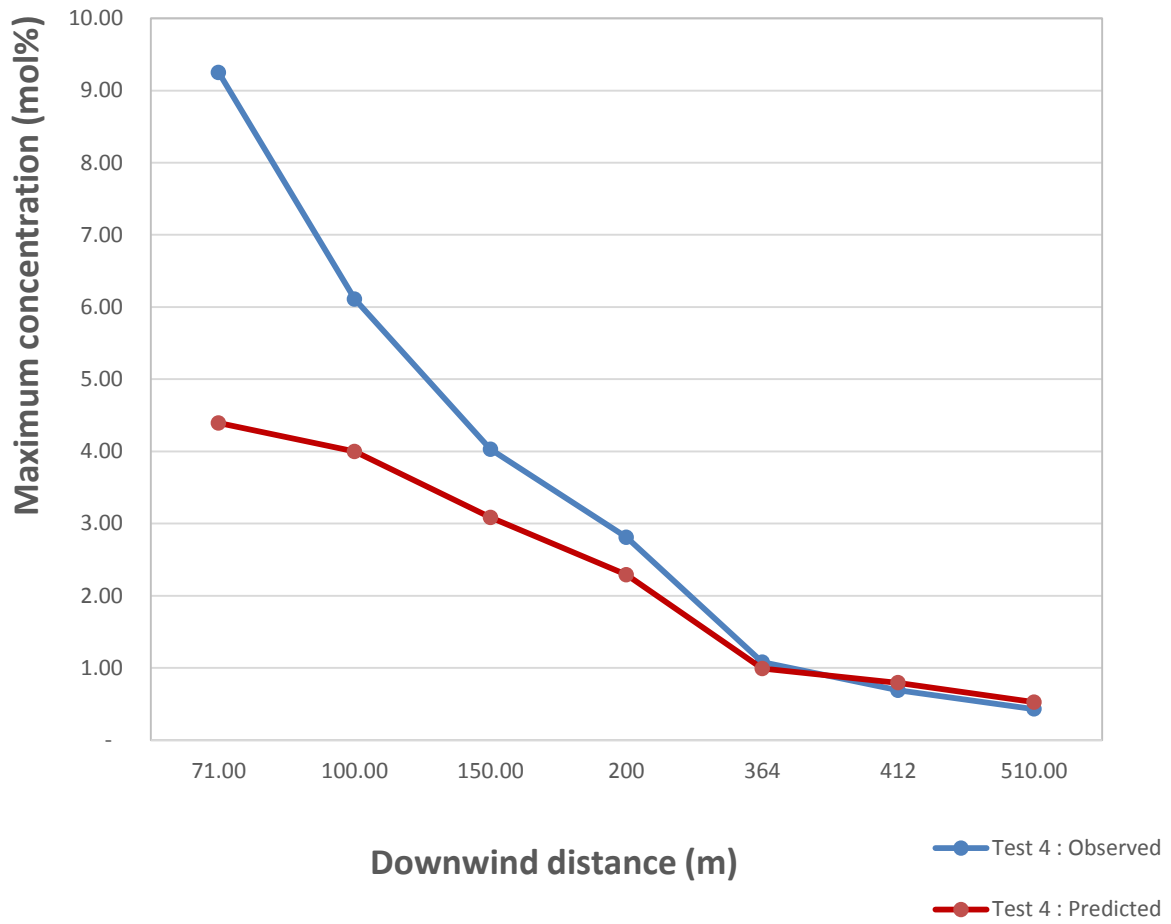
Test 4:

C = 1.00

 $\alpha^* = 0.50$ $\alpha = 0.60$ $U^*/U = 0.10$

X(m)	T(s)	t_ind ex	gas conc.	gas M (kg/ mol)	gas conc mol	r	h	ma	v	rho air	air M (kg/ mol)	air conc.	mol %	obser ved mol%	error %
71	29.9	300	0.22060	120	0.001838	95.43	1.31800	43,750	37,708.14	1.16	29	0.04001	4.39	9.25	(110.56)
100	41.7	418	0.20290	120	0.001691	120.80	1.13400	61,210	51,987.24	1.18	29	0.04060	4.00	6.11	(52.82)
150	61.9	620	0.15720	120	0.001310	161.00	0.97770	95,050	79,617.26	1.19	29	0.04117	3.08	4.03	(30.67)
200	83.9	840	0.11680	120	0.000973	202.40	0.90340	140,000	116,265.53	1.20	29	0.04152	2.29	2.81	(22.68)
364	151.9	1,520	0.05032	120	0.000419	326.40	0.87870	357,700	294,097.14	1.22	29	0.04194	0.99	1.08	(9.10)
412	171.9	1,720	0.04031	120	0.000336	363.00	0.89410	451,000	370,125.68	1.22	29	0.04202	0.79	0.69	13.00
510	212.9	2,130	0.02665	120	0.000222	439.40	0.94	694,300	568,766.35	1.22	29	0.04209	0.52	0.43	18.07

Observed and predicted maximum concentration at various downwind distances for Test 04



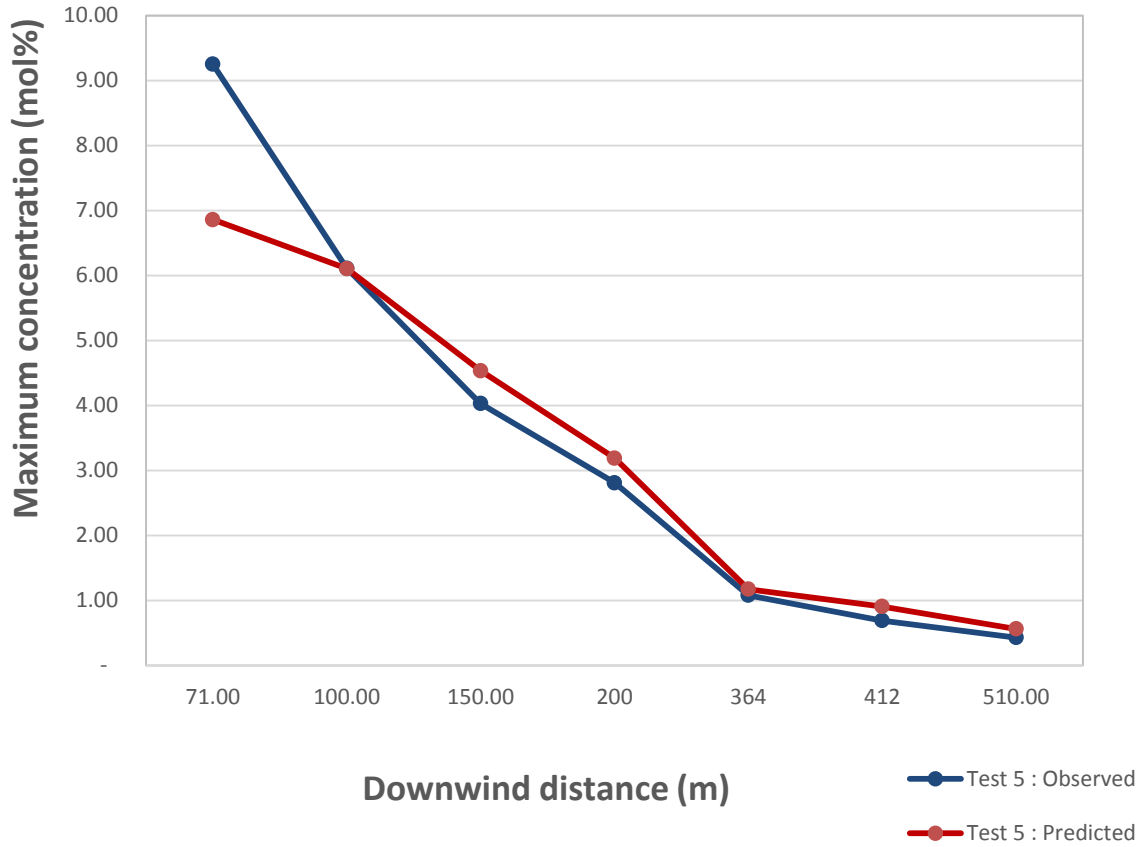
Test 5:

C = 1.30

 $\alpha^* = 0.50$ $\alpha = 0.50$ $U^*/U = 0.10$

X(m)	T(s)	t_ind ex	gas conc.	gas M (kg/ mol)	gas conc mol	r	h	ma	v	rho air	air M (kg/ mol)	air conc.	mol%	obser ved mol%	error %
71	29.9	300	0.34420	120	0.002868	101.30	0.80560	29,330	25,970.97	1.13	29	0.03894	6.86	9.25	(34.84)
100	41.7	418	0.31090	120	0.002591	127.00	0.69480	40,680	35,206.04	1.16	29	0.03984	6.11	6.11	(0.08)
150	61.9	620	0.23200	120	0.001933	168.20	0.61840	64,880	54,963.11	1.18	29	0.04070	4.53	4.03	11.12
200	83.9	840	0.16300	120	0.001358	211.60	0.59950	100,800	84,327.73	1.20	29	0.04122	3.19	2.81	11.92
364	151.9	1,520	0.05966	120	0.000497	347.30	0.65870	303,200	249,601.45	1.21	29	0.04189	1.17	1.08	7.93
412	171.9	1,720	0.04611	120	0.000384	388.80	0.68650	396,800	326,019.01	1.22	29	0.04197	0.91	0.69	23.95
510	212.9	2,130	0.02856	120	0.000238	476.60	0.74700	650,500	533,063.01	1.22	29	0.04208	0.56	0.43	23.54

Observed and predicted maximum concentration at various downwind distances for Test 05



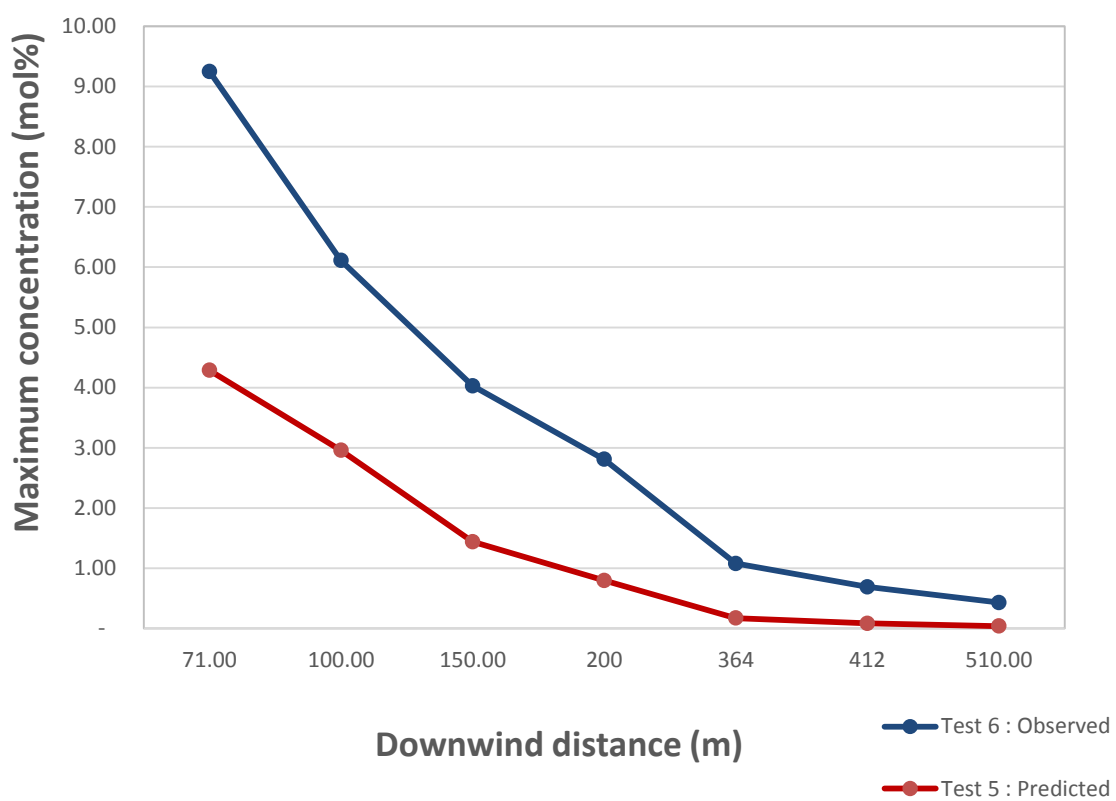
Test 6:

C = 1.30

 $\alpha^* = 0.50$ $\alpha = 0.50$ $U^*/U = 0.20$

X(m)	T(s)	t_index	gas conc.	gas M (kg/mol)	gas conc mol	r	h	ma	v	rho air	air M (kg/mol)	air conc.	mol %	observed mol%	error %
71	29.9	300	0.21670	120	0.001806	107.90	1.20400	51,480	44,037.15	1.169013	29	0.04031	4.29	9.25	(115.73)
100	41.7	418	0.15050	120	0.001254	140.90	1.24700	92,760	77,774.69	1.192676	29	0.04113	2.96	6.11	(106.47)
150	61.9	620	0.07440	120	0.000620	199.60	1.39600	215,000	174,725.53	1.230501	29	0.04243	1.44	4.03	(179.83)
200	83.9	840	0.04047	120	0.000337	267.50	1.58400	433,800	356,084.13	1.218251	29	0.04201	0.80	2.81	(252.83)
364	151.9	1,520	0.00883	120	0.000074	502.70	2.14900	2,088,000	1,706,098.33	1.223845	29	0.04220	0.17	1.08	(520.62)
412	171.9	1,720	0.00428	120	0.000036	578.30	2.30500	2,963,000	2,421,738.17	1.223501	29	0.04219	0.08	0.69	(716.12)
510	212.9	2,130	0.00205	120	0.000017	741.00	2.60900	5,510,000	4,500,495.87	1.224310	29	0.04222	0.04	0.43	(963.60)

Observed and predicted maximum concentration at various downwind distances for Test 06



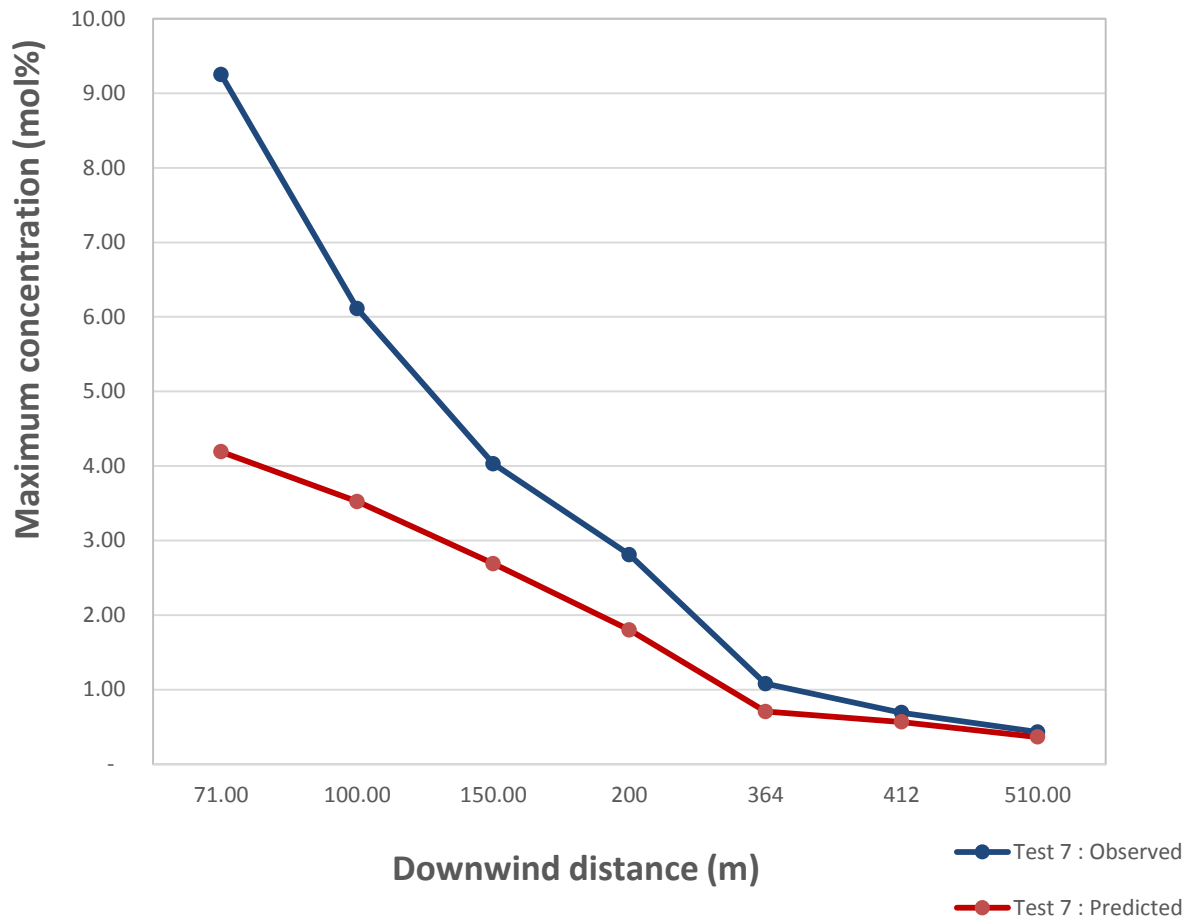
Test 7:

C = 1.30

 $\alpha^* = 0.50$ $\alpha = 0.60$ $U^*/U = 0.10$

X(m)	T(s)	t_ind ex	gas conc.	gas M (kg/ mol)	gas conc mol	r	h	ma	v	rho air	air M (kg/ mol)	air conc.	mol %	obser ved mol%	error %
71	29.9	300	0.21240	120	0.001770	114.60	1.15100	55,740	47,489.15	1.173742	29	0.04047	4.19	9.25	(120.77)
100	41.7	418	0.17990	120	0.001499	145.40	0.99460	78,660	66,058.26	1.190767	29	0.04106	3.52	6.11	(73.46)
150	61.9	620	0.13740	120	0.001145	194.60	0.87040	124,400	103,551.03	1.201340	29	0.04143	2.69	4.03	(49.83)
200	83.9	840	0.09177	120	0.000765	245.60	0.81660	187,100	154,744.77	1.209088	29	0.04169	1.80	2.81	(56.01)
364	151.9	1,520	0.03589	120	0.000299	400.30	0.82370	505,500	414,658.07	1.219077	29	0.04204	0.71	1.08	(52.88)
412	171.9	1,720	0.02868	120	0.000239	446.60	0.84440	645,500	529,097.29	1.220002	29	0.04207	0.56	0.69	(22.14)
510	213.9	2,130	0.01843	120	0.000154	543.30	0.89600	1,015,000	830,878.06	1.221599	29	0.04212	0.36	0.43	(18.37)

Observed and predicted maximum concentration at various downwind distances for Test 07



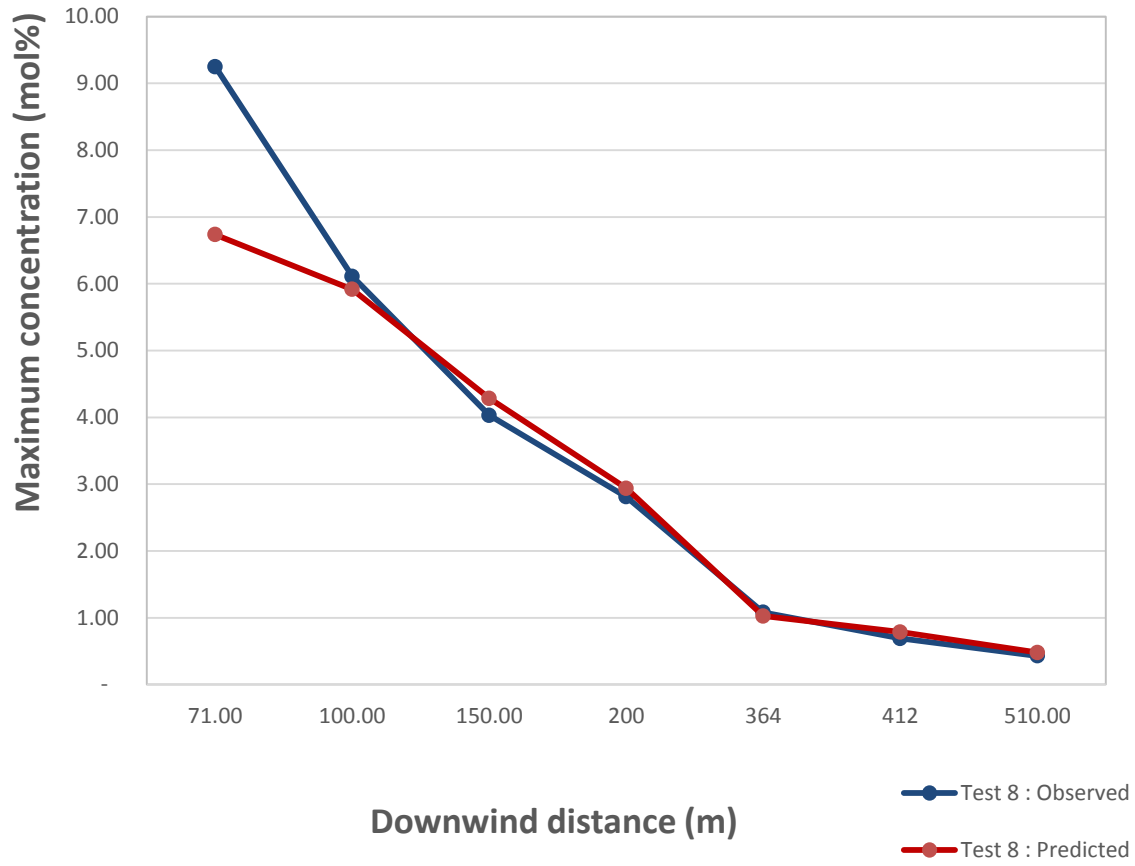
Test 8:

C = 1.00

 $\alpha^* = 0.60$ $\alpha = 0.50$ $U^*/U = 0.10$

X(m)	T(s)	t_index	gas conc.	gas M (kg/mol)	gas conc mol	r	h	ma	v	rho air	air M (kg/mol)	air conc.	mol %	observed mol %	error %
71	29.9	300	0.33820	120	0.002818	101.50	0.81850	29,980	26,491.14	1.131699	29	0.03902	6.74	9.25	(37.33)
100	41.7	418	0.30120	120	0.002510	127.50	0.71380	42,200	36,454.13	1.157619	29	0.03992	5.92	6.11	(3.28)
150	61.9	620	0.21900	120	0.001825	169.50	0.64740	69,080	58,433.51	1.182198	29	0.04077	4.28	4.03	5.95
200	83.9	840	0.15000	120	0.001250	214.00	0.63840	110,000	91,848.13	1.197629	29	0.04130	2.94	2.81	4.35
364	151.9	1,520	0.05215	120	0.000435	355.20	0.72180	348,000	286,096.58	1.216372	29	0.04194	1.03	1.08	(5.32)
412	171.9	1,720	0.03992	120	0.000333	398.70	0.75550	459,700	377,291.32	1.218422	29	0.04201	0.79	0.69	12.17
510	212.9	2,130	0.02434	120	0.000203	491.00	0.83	764,900	626,351.85	1.22	29	0.04211	0.48	0.43	10.30

Observed and predicted maximum concentration at various downwind distances for Test 08



Test 9:

$C = 1.3$

$\alpha^* = 0.70$

$\alpha = 0.50$

$U^*/U = 0.10$

X(m)	T(s)	t _{index}	gas conc.	gas M (kg/mol)	gas conc mol	r	h	ma	v	rho air	air M (kg/mol)	air conc.	mol%	observed mol%	error %
71	29.9	300	0.3323	120	0.002769	101.70	0.83120	30,620	27,008.30	1.133725	29	0.03909	6.61	9.25	(39.84)
100	41.7	418	0.2921	120	0.002434	128.00	0.73240	43,710	37,697.99	1.159478	29	0.03998	5.74	6.11	(6.47)
150	61.9	620	0.2074	120	0.001728	170.70	0.67570	73,280	61,854.43	1.184717	29	0.04085	4.06	4.03	0.71
200	83.9	840	0.1390	120	0.001158	216.30	0.67590	119,300	99,344.85	1.200867	29	0.04141	2.72	2.81	(3.26)
364	151.9	1,520	0.0463	120	0.000386	362.60	0.78180	393,200	322,924.61	1.217622	29	0.04199	0.91	1.08	(18.66)
412	171.9	1,720	0.0351	120	0.000293	408.00	0.82100	523,300	429,351.87	1.218814	29	0.04203	0.69	0.69	0.28
510	212.9	2,130	0.0212	120	0.000176	504.30	0.90280	881,100	721,305.69	1.221535	29	0.04212	0.42	0.43	(3.15)

Observed and predicted maximum concentration at various downwind distances for Test 09

